

Seismogenic, Electrically Conductive, and Fluid Zones at Continental Plate Boundaries in New Zealand, Himalaya, and California-USA

George R. Jiracek¹, Victor M. Gonzalez¹, T. Grant Caldwell²,
Philip E. Wannamaker³, and Debi Kilb⁴

We explore the idea that fluid occurrence below the seismogenic zone plays an active role in the rupture process by examining how fluids spatially relate to seismicity at three continental plate boundaries: South Island of New Zealand, the Himalaya, and San Andreas fault, USA. With this objective, we project earthquake hypocenters onto magnetotelluric (MT) electrical resistivity cross-sections. MT detection of conductive zones in the crust containing low fractions of fluids (<1%) requires an interconnected network of fluid-filled porosity facilitated by shearing, fracturing, and/or grain-edge wetting. Mechanisms promoting fluid reservoirs in the ductile crust include: 1) stalling of upward propagating porosity waves, 2) tectonically induced neutral buoyancy, and 3) development of ductile shear zones. Distinct conductive horizons are detected at depth in the ductile crust in New Zealand and the Himalaya where the tectonic convergence is high. In the Parkfield segment of the San Andreas fault, where convergence is low, there is high conductivity in the ductile crust but it forms a sub-vertical corridor to the surface with no distinct top. The tops of sub-horizontal conductive zones are ~20 km depth in New Zealand and ~25–40 km in the Himalaya where the seismogenic crust extends only to 12 and 25 km depth, respectively. The deep conductive layer in New Zealand may have originated as a “water sill” facilitating water-weakening, localized deformation, and eventually becoming a water-rich, anisotropic, mylonized, ductile shear zone. Fluid exchange through the active Alpine fault may initiate or be initiated by fault rupture. Localized, unstable flow in deep fluidized zones detected by MT may trigger earthquakes above.

1. INTRODUCTION

Understanding the dynamics of earthquake rupture remains a critically important role of science in human society. However, the physical-chemical processes that lead to earthquake nucleation and rupture remain elusive. There is increasing evidence that processes removed from the actual seismogenic zone may be very important. For example, in Japan *Iio and Kobayashi* [2002] suggested that accelerated aseismic slip on a shear zone in the lower ductile crust triggered a major earthquake on a steeply dipping fault in the upper brittle crust. *Rogers and Dragert* [2003] proposed that stress loading evidenced by deep non-earthquake signals monitored in the

Supplemental Information is available at: http://eqinfo.ucsd.edu/~dkilb/Jiracek/Jiracek_web.html.

¹Department of Geological Sciences, San Diego State University, San Diego, California.

²GNS Science, Lower Hutt, New Zealand.

³Energy & Geoscience Institute, University of Utah, Salt Lake City, Utah.

⁴Scripps Institution of Oceanography, University of California, San Diego, La Jolla, California.

A Continental Plate Boundary. Tectonics at South Island, New Zealand Geophysical Monograph Series 175
10.1029/175GM18

Cascadia subduction zone could affect the locked portion of a fault, thereby triggering a large thrust earthquake. In California, USA, *Nadeau and Dolenc* [2005] discovered nonvolcanic tremor activity at 20 to 40 km below the San Andreas fault that correlates in space and time with local earthquake activity in the overlying, 15-km-thick, seismogenic crust. In all of these cases the authors have suggested fluid-related processes well below the seismogenic zone as the origin of stress increase in the upper brittle crust.

Before proceeding, we define three terms that will be used repeatedly. First, the brittle, seismogenic portion of the crust will mean the uppermost region where the localized frictional strength or resistance to shear increases linearly with depth in a manner often described as *Byerlee* [1978] behavior. Second, below the brittle section we define the ductile portion of the crust to be the increasingly weaker lower crust which undergoes aseismic, power law distributed creep. This depth profile of crustal rheology characterizes the famous “pine-tree plot” of crustal strength versus depth [e.g., *Sibson*, 1984]. Third, we use the common usage of the term brittle-ductile transition to be the transition between the upper seismogenic crust and the creeping section below.

The “standard” description of the crust of localized friction (brittle behavior) above to broadly distributed creep (ductile behavior) below is called the “older concept” by *Rice and Cocco* [2007]. They cite a “more recent concept” where the transition is from potentially unstable to inherently stable, but still localized, friction. The base of the seismogenic zone is the transition between the two modes of localized friction rather than a transition from localized friction to distributed creep. Since this model assumes localized deformation at all levels, *Rice and Cocco* [2007] pointed out a difficulty by suggesting that below the seismogenic zone there could be broadly distributed deformation during the interseismic period but localized deformation during deeply penetrating earthquake rupture. *Hobbs et al.* [2002] prefer the terms plastic (pressure sensitive/temperature insensitive) and viscous (pressure insensitive/temperature sensitive) instead of brittle and ductile, respectively. A viscous material is usually highly ductile but it can exhibit localized deformation, and a plastic material can be brittle or ductile depending on the conditions of deformation [*Hobbs et al.*, 2002]. Independent of what mechanism is used to describe the “brittle-ductile transition,” there is a temperature limit for the depth of seismogenesis (e.g., ~350°C for wet granite) and continued interseismic creep occurs below the locked seismogenic zone [*Rice and Cocco*, 2007].

The San Andreas fault observatory at depth (SAFOD) experiment in California, USA seeks to characterize the uppermost portion of an active fault zone by drilling into it, sampling and monitoring it. The SAFOD program used an array of geophysical measurements including seismic reflec-

tion and tomography, gravity and magnetic surveys, micro-earthquake monitoring, and magnetotelluric (MT) soundings to locate the drill site. The ability of the MT method to image very low interconnected fractions (<1%) of aqueous fluid [e.g., *Wannamaker et al.*, 2002] proved valuable in evaluating the hydrologic conditions in uppermost brittle crust of the SAFOD site [*Unsworth and Bedrosian*, 2004a]. It has been accepted for some time that the redistribution of fluids in seismic fault zones can trigger shallow earthquakes [e.g., *Nur and Booker*, 1972; *Rice*, 1992; *Sibson*, 1992; *Byerlee*, 1993; *Hickman et al.*, 1995; *Gratier et al.*, 2003] and there is evidence that interconnected pore fluid is ubiquitous throughout the seismogenic zone [e.g., *Fialko*, 2004]. However, the idea that fluid concentration and movement below the seismogenic zone plays an active role in the earthquake cycle is relatively new. In 1995 *Hickman et al.* [1995] posed the question “are fluids present in the sub-seismogenic crust?” Since then the evidence has been overwhelming leading *Ague* [2006] to state in an invited address at the American Geophysical Union’s 2006 Spring Assembly that “the presence of fluids in deep settings is no longer in dispute.” The presence of fluid in the deep crust influences the rheological properties; in particular, it can dramatically reduce the shear strength [e.g., *Cox*, 2005]. However, the response of the ductile crust to increased fluid content is not unique since increasing the geothermal gradient, changing the rock composition to more quartz-rich or less feldspar rich, or decreasing the strain rate all have the same effect on crustal strength versus depth [*Sibson*, 1984]. Finally, the fate of the fluid, especially how it affects the earthquake cycle, involves a complex, nonlinear coupling between thermal, chemical, mechanical, and hydrological processes.

Despite the recognition of the importance of fluids in the earthquake nucleation process, there are many critical unanswered questions such as their origin, transport, and storage. Another fundamental question is how does the spatial distribution of fluids relate to seismicity in active tectonic settings? We will attempt to answer this question for three major continental plate boundaries emphasizing the origin, movement, and accumulation at or below the brittle-ductile transition. A first order requirement is to locate and understand anomalous zones of aqueous fluid and/or partial melt concentrations in the ductile regions of active, earthquake prone areas. From the beginning we will assume, as have many before [e.g., *Gough*, 1986; *Jiracek et al.*, 1983, 1995; *Marquis and Hyndman*, 1992; *Wei et al.*, 2001; *Wannamaker et al.*, 2002; *Unsworth and Bedrosian*, 2004a, 2004b; *Ritter et al.*, 2005], that MT imaging of most crustal conductive features in active settings is mapping zones of interconnected, fluids (either aqueous or partial melt). The three regions we have chosen to study are locations of varying degrees of compressional, continental plate boundaries: 1)

the Southern Alps in New Zealand, 2) the Himalaya, and 3) a “transitional” portion of the San Andreas fault. Distinct differences in tectonic style, particularly the rate and scale of convergence, influence fluid generation, migration, and occurrence of the electrically conductive features and their relationship to deformation processes. Ultimately we seek a dynamic coupling between high conductivity regions [fluids] and earthquake occurrences.

It is important to understand that not all features of deep conductive zones are well-resolved by the MT method. However, in the usual case where the MT wavelengths (or skin depths) are large compared to the thickness of such layers, there are two quantities that are well-resolved. These are [e.g., *Jiracek et al.*, 1995]: 1) the depth to the top of the conductor and 2) its vertically integrated conductivity or conductance, namely, the conductivity-thickness product (or, equivalently, the thickness over resistivity quotient since resistivity is the reciprocal of the conductivity). Consequently, when comparing crustal conductive zones, we will stress the depth to the top and their conductance. A requirement for MT detection of any layer-like conductive feature is that its conductance significantly exceeds the integrated conductance of the entire overlying crust.

We will review briefly the tectonic settings of the three study areas and compare and contrast the patterns of seismicity and conductivity, the latter inferring zones of fluid concentration in the ductile portion of the crust. Following the reviews we outline key results from the literature on the origin and fate of deep metamorphic fluids and the formation of fluid reservoirs below, or at, the brittle-ductile transition. In particular, fluid-filled fracture development and grain-edge wetting are discussed since fluids must be interconnected over tens of kilometers for detection by MT at mid-crustal depths. The requirement of sustained permeability in the ductile crust leads us to conclude that pervasive ductile shear zones may trap fluids and explain the high conductivity, an idea proposed decades ago by *Eaton* [1980]. Finally, possible links between earthquakes and the deep fluids (particularly aqueous) are proposed. Results from recent publications on crustal-scale fluid distribution in compressive tectonic environments also will be reviewed as they relate to our objectives. Details of the MT and earthquake data collection and modeling in the three study areas are not addressed herein since they are well-described in the literature cited below.

2. PLATE BOUNDARY STUDY AREAS—CONDUCTIVE AND SEISMOGENIC ZONES

2.1. New Zealand

South Island of New Zealand has been the focus of our group for over 10 years [*Wannamaker et al.*, 2002] so we

present original MT results from this area along with a more complete analysis. Our MT work began with a pilot study of only 12 soundings in 1995 as part of an extensive multi-disciplinary, continental dynamics project [*Davey et al.*, 1998]. Few MT soundings had been recorded previously across the Southern Alps that dominate the striking topography of the central, 150 to 200-km-wide, portion of South Island. Here, the ~37 mm/yr displacement between the Pacific and Australian plates [*DeMets et al.*, 1994] is manifested by a 500-km-long mountain range with peaks rising to in excess of 3750 m. A convergent component of the orogen developed about 5-6 Ma ago and has resulted in ~70 km of shortening, crustal thickening, and exhumation of ~25-km-deep metamorphic rocks (Figure 1) along a ~50° southeast dipping, plate boundary fault called the Alpine fault [*Walcott*, 1998; *Norris*, 2004]. The Alpine fault accommodates most of the oblique plate motion between a strong Australian plate and a weaker Pacific plate (Figure 1). Convergence in the central segment of the Alpine fault is estimated to be about 10 mm/yr and there is ~35 mm/yr slip rate parallel to the fault [*Norris*, 2004; *Beavan et al.*, this volume]. We collected 54 MT soundings in 1995–1998 across the central segment including sites occupied over the 30-km-wide, rugged main divide of the Southern Alps using helicopter support. Detailed results of this effort appear in *Gonzalez* [2002] and *Wannamaker et al.* [2002].

For this study we use the 150-km-long two-dimensional (2-D) resistivity model (Plate 1) presented by *Gonzalez* [2002]. It differs slightly from that presented by *Wannamaker et al.* [2002] because *Gonzalez* [2002] applied near-surface distortion analysis [*Groom and Bailey*, 1989]. The model was derived using the 2-D MT inversion algorithm of *Rodi and Mackie* [2001] using the cross-strike, electric field response function (the transverse magnetic, TM mode). Inversion using both the TM and the along strike electric field response (the transverse electric, TE mode) produced a markedly different resistivity image due to partial violation of the 2-D assumption and significant anisotropy [*Gonzalez*, 2002; *Wannamaker et al.*, 2002]. However, the depth to the top of the deep conductor of ~20 km is in agreement. In three-dimensional (3-D) circumstances, a 2-D inversion using the TM mode alone gives results in better agreement with the actual resistivity cross-section perpendicular to the long axis of a buried 3-D conductive body [*Wannamaker et al.*, 1984; *Ledo*, 2005]. Such geometry has been established for the conductive body under the Southern Alps by additional MT soundings extending tens of km either side of the MT line marked in Figure 1. Resistivity values in Plate 1 span a large range from very highly resistive (10^4 ohm m and greater) to conductive (~10 ohm m). We stress that it is the depth to the top of the deep conductor (~20 km) and its conductance

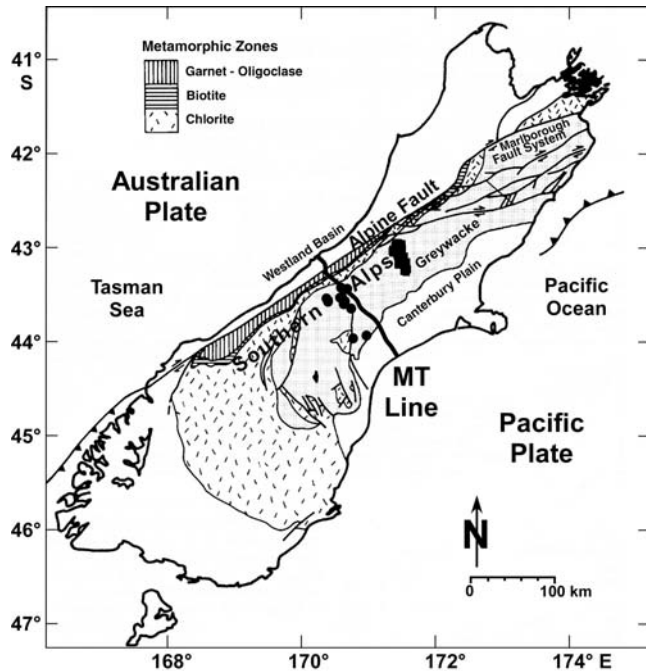


Figure 1. Location map of MT line across South Island of New Zealand. Metamorphic zones after Vry *et al.* [2001] and references therein. Epicenter locations from Eberhart-Phillips and Bannister [2002] (black dots) and Bannister *et al.* [2006] (black squares).

that are the best resolved quantities not its actual resistivity. Conductance calculations for the deep conductor in the ductile portion of the crust in Plate 1 range from 50 S in the cross-strike direction to 500 S in the along-strike direction. This electrical anisotropy is attributed to active, shearing in the fluidized zone of the ductile crust caused by plate motion [Wannamaker *et al.*, 2002].

Our focus in this paper is mainly on the conductive zone (imaged as ≤ 200 ohm m in the resistivity model) traced laterally from approximately 60 km southeast of the Alpine fault (Plate 1) to ~ 5 – 10 km southeast of the fault proper. Over this span, the conductive zone rises on both ends from a depth to its top of ~ 20 km under the eastern foothills of the Southern Alps. To the northwest it slopes sharply upward, nearly paralleling the depth projection of the Alpine fault, before it rises almost vertically from ~ 10 km depth (Plate 1). It intersects the surface at 5 – 10 km southeast of the fault trace. Wannamaker *et al.* [2002] note that 10 km depth is approximately at the brittle-ductile transition as established by others [e.g., Beavan *et al.*, 1999; Leitner *et al.*, 2001]. Where the conductor also rises to the surface ~ 60 km southeast of the Alpine fault the modeled conductivity, and therefore conductance, is more than an order of magnitude less

than that associated with the Alpine fault strand (Plate 1). A conductive outcrop and two upward extending conductive limbs at ~ 60 to 75 km distance in Plate 1 are coincident with mapped locations of backthrust faults associated with crustal shortening and uplift of the Southern Alps [Cox and Findlay, 1995]. Wannamaker *et al.* [2002] concluded that the origin of the fluids inferred to cause the high conductivity ~ 20 km beneath the Southern Alps lies mainly in the release of aqueous fluid from prograde metamorphism in a thickened crustal root. They estimated the amount of saline fluid to be ~ 0.02 – 0.2% where the resistivity is ~ 100 ohm m and 0.2 to 3% where the resistivity is lower (~ 10 ohm m). Since the top of the deep conductor is at ~ 20 km depth, it is well below the brittle-ductile transition of ~ 12 km [Leitner *et al.*, 2001] so the deepest fluids probably interconnect through grain-edge wetting [e.g., Holness, 1993; Spear, 1993] within a ductile shear zone [Tullis *et al.*, 1996] rather than in fractures.

There is a unique opportunity to evaluate the nature of the deep crustal conductive zone beneath the Southern Alps because exhumation along the hanging wall of the Alpine fault has exposed a sequence of rocks from over 20 km depth [Norris, 2004]. Near the fault, i.e., at the deepest part of the exhumed sequence, is a mylonite zone that shows very large shear strain, intense strain localization, and mineral assemblages that indicate deformation under metamorphic conditions at depths of 20 – 30 km [Grapes and Watanabe, 1994; Vry *et al.*, 2004]. Norris [2004] believes the mylonites formed during the last 5 Myr since plate convergence began and reactivation of an older discontinuity developed along the Alpine fault. Ductile shear recorded by the mylonites supports the projection of the Alpine fault via ductile creep to depths of the midcrustal conductor. Therefore, the preponderance of evidence lead us [Wannamaker *et al.*, 2002] to conclude that the ~ 20 -km-deep conductor lies in an active, mylonized, ductile shear zone where deep-sourced fluids are trapped. Additional fluids may be released by strain-induced metamorphism [Koons *et al.*, 1998; Upton *et al.*, 2003; Upton and Koons, this volume] and shearing itself promotes deformation-enhanced grain boundary wetting and fluid interconnection [Tullis *et al.*, 1996; Cox, 2005]. Shear interconnection also explains the strong resistivity anisotropy below central South Island, because the greater degree of shear along strike promotes long-range “backbone” (connected) shears in that direction [Cox, 2005; Wannamaker, 2005]. The fluids in the ductile shear zone may have developed initially as a “water sill” (see Section 3).

The seismicity of the Alpine fault and the Southern Alps in New Zealand has been the focus of several recent efforts that have produced high quality hypocenter data [Eberhart-Phillips, 1995; Leitner *et al.*, 2001; Eberhart-Phillips and Bannister, 2002; Bannister *et al.*, 2006]. These data show

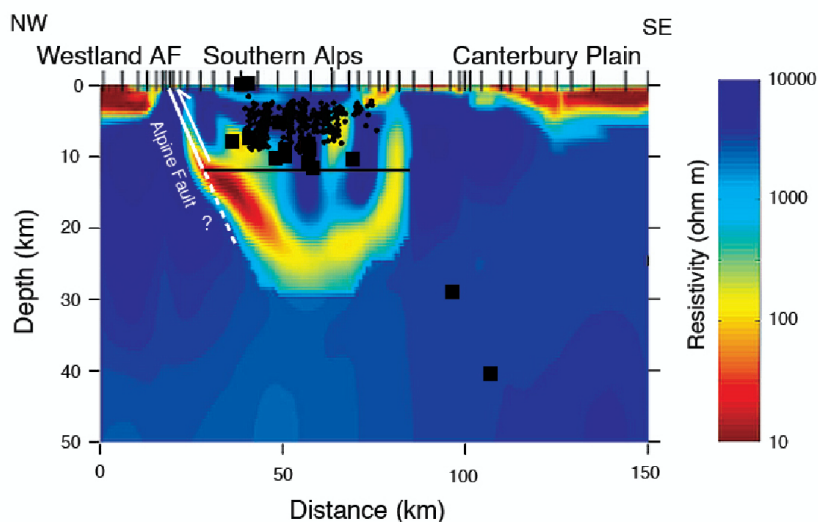


Plate 1. Electrical resistivity model of New Zealand MT line [Gonzalez, 2002]. Vertical ticks are locations of MT sites. AF denotes surface location of the Alpine fault; projection to depth assumes 50° SE dip. Black squares are earthquake hypocenters with magnitudes 2.0 to 3.9 occurring within ± 15 km of the MT profile [Eberhart-Phillips and Bannister, 2002] and black dots are locations of 1994 $M_w = 6.7$ Arthur's Pass earthquake and 40 aftershocks [Bannister et al., 2006] projected parallel to the Alpine fault (Figure 1). Horizontal black line at 12 km depth marks brittle-ductile transition [Leitner et al., 2001].

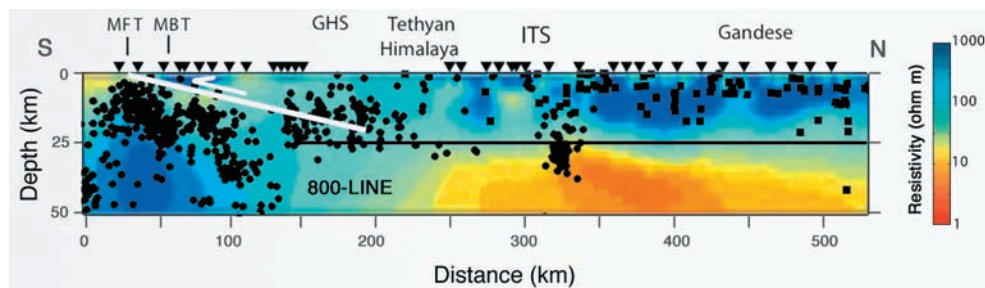


Plate 2. Electrical resistivity model for the Himalaya MT 800-line+Nepal from Unsworth et al. [2005]. Inverted triangles indicate MT stations. Abbreviations are: MFT (Main Frontal thrust), MBT (Main Boundary thrust), GHS (greater Himalaya sequence), and ITS (Indus–Tsangpo suture). Black circles are hypocenters from Schulte-Pelkum et al. [2005] and black squares are hypocenters from Langin et al. [2003] and Monsalve et al. [2006]. The extension of MFT corresponds to the shear zone presented by Schulte-Pelkum et al. [2005]. The black horizontal line at 25 km depth marks the brittle-ductile transition [Langin et al., 2003].

that the base of the seismogenic zone is at 12 ± 2 km in the central part of the Southern Alps; ~ 10 km above the top of the midcrustal conductor shown in Plate 1. Here, the positions of nearby, accurately located hypocenters from these studies are projected parallel to strike onto the resistivity model. Shown are hypocenters from 17 earthquakes having local magnitudes ranging from 2.0 to 3.9, occurring during 1979–1996, all within 15 km of the MT profile [Eberhart-Phillips and Bannister, 2002], and the locations of the 1994 $M_w = 6.7$ Arthur's Pass earthquake and 40 aftershocks [Bannister *et al.*, 2006]. Epicenter locations for these earthquakes are presented in Figure 1. Although the 1994 sequence is ~ 70 km from the MT profile it is included here since the lateral and depth extent of the seismogenic zone is thought to be nearly uniform in this part of central South Island [Leitner *et al.*, 2001]. Moreover, this is the most reliable, detailed image of a moderate earthquake and its aftershock sequence associated with the Southern Alps. Nearly all of the seismic activity in this region occurs inboard (southeast) of the Alpine fault (Figure 1 and Plate 1) in a broad region of brittle deformation best modeled by numerous north-northeast trending reverse faults [Leitner *et al.*, 2001]. Earthquake focal mechanisms indicate significant components of dip slip (compression) and strike-slip, as expected. The comparatively low seismicity rate measured over the last 150 years indicates that only a small fraction of the strain accumulation has been released; this is interpreted to indicate the potential for large earthquakes along the Alpine fault [Leitner *et al.*, 2001].

A deeper northwest-dipping seismicity zone in this region of South Island defines a diffuse pattern that crosses the brittle-ductile transition and into the stiff upper mantle of the Pacific Plate [Liu and Bird, 2006]. The southernmost epicenters in Figure 1 and the corresponding hypocenters in Plate 1 at ~ 31 and 43 km depth are in this zone.

2.2. Himalaya

There have been several recent MT surveys across the Himalaya, specifically across the Indus-Tsangpo suture (ITS), also called the Yarlung-Tsangpo suture (YTS), in southern Tibet that divides rocks of Indian and Asian origin [e.g., Wei *et al.*, 2001; Spratt *et al.*, 2005; Unsworth *et al.*, 2005]. Underthrusting of the Indian continental lithosphere under Eurasia has resulted in the stacking of several crustal-scale thrust sheets [e.g., Beaumont *et al.*, 2001; DeCelles *et al.*, 2002] and a doubling of the crustal thickness to ~ 80 km [Owens and Zandt, 1997]. Convergence of India and Eurasia from global positioning system (GPS) measurements is 36–40 mm/yr; 15–20 mm/yr occurs within the Himalaya [Zhang *et al.*, 2004].

We have selected the MT 800-line+Nepal profile as representative of the MT results presented by Unsworth *et al.*

[2005]. It traces a prominent crustal conductor for the greatest distance (>300 km) [Plate 2]. The Nepal portion of this profile (the southern ~ 170 km in Plate 2) was described earlier by Lemonnier *et al.* [1999]. They believe that the ~ 20 -km-deep, ~ 30 ohm m conductive occurrence, and seismicity, near the downward terminus of the line representing the Main Frontal fault in Plate 2 is caused by fluids released from metamorphic reactions in the footwall of the thrust.

There is remarkable agreement of the salient geoelectric features from the four MT lines presented by Unsworth *et al.* [2005] even though they are spread over 1000 km distance. Location of these lines is mapped in Figure 2. Lowest resistivity zones (≤ 10 ohm m) are imaged north of the Tethyan Himalaya on each geoelectric profile with tops at ~ 25 to 40 km depth [e.g., Plate 2; Unsworth *et al.*, 2005]. The conductance of these zones is highest in the vicinity of the ITS, at $\sim 20,000$ S, and exceeds 1000 S for hundreds of km north [Wei *et al.*, 2001]. This is over an order of magnitude greater conductance than the deep conductor under the Southern Alps of New Zealand. Unsworth *et al.* [2005] interpreted this conductive zone as an interconnected, 5 to 14% partial melt fraction. Makovsky and Klempere [1999] and Li *et al.* [2003] suggested that the nature of reflection seismic bright spots combined with the electrical conductivity favor an interpretation with both saline water and partial melt. The resulting conductive zone is estimated to have the equivalent of ~ 200 m of saline fluid above ~ 10 km thickness of $\sim 10\%$ partial melt. Klempere [2006] believes this sequence best fits a picture of fluid rising from the subducting Indian subcontinent and triggering partial melting of granite at temperatures of $\sim 650^\circ\text{C}$ resulting from radiogenic heating. We would add that fluid production and possible melting would be enhanced by the crustal thickening itself in a fashion analogous to, but greater than, crustal development under the Southern Alps. Klempere [2006] emphasizes that if either water or melt are present, the effect is a region of weak crust that would allow midcrustal flow that decouples the upper and lower parts of the crust under southern Tibet [Nelson *et al.*, 1996; Royden *et al.*, 1997; Schulte-Pelkum *et al.*, 2005]. Unsworth *et al.* [2005] estimate that the reduced viscosity calculated from the melt fraction required by the MT data is consistent with such midcrustal flow in southern Tibet.

Seismicity north of the ITS in central Tibet was evaluated by Langin *et al.* [2003] as part of the 1998–99 INDEPTH III program (International Deep Profiling of Tibet and Himalaya). Using a histogram of the focal depths (Figure 3) the authors concluded that 99% of the events are at depths shallower than 25 km in central Tibet. Langin *et al.* [2003] cited these data, along with MT data, as indicating that the crust in this region below the ~ 25 km level is undergoing ductile, aseismic deformation, and mid to deep crustal flow. The fo-

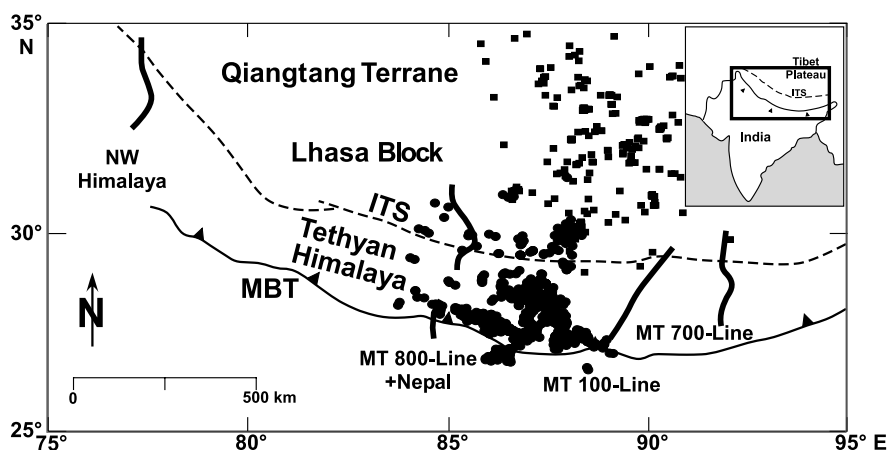


Figure 2. Location map of MT profiles crossing the Himalayan Indus-Tsangpo suture (ITS) and the Tibetan plateau. MT 800-line+Nepal is used in this paper. MBT is the Main Boundary thrust. Modified from *Unsworth et al.* [2005] and *Klemperer* [2006]. Epicenter locations from *Langin et al.* [2003], *Schulte-Pelkum et al.* [2005], and *Monsalve et al.* [2006].

cal mechanisms in the brittle 25-km-deep seismogenic crust are consistent with the north-south compression produced by India-Eurasia collision. The hypocenter data from *Langin et al.* [2003] are projected onto the MT 800-line+Nepal geoelectric section in Plate 2 as are the surface positions of the Main Boundary thrust (MBT) and the Main Frontal thrust (MFT) (with its projection downward). To provide additional coverage, particularly south of the ITS, we have included additional hypocenter data recently published by *Schulte-Pelkum et al.* [2005] and *Monsalve et al.* [2006] recorded in Nepal and Tibet in 2001–2003. Epicenter loca-

tions of all earthquake events used in Plate 2 are shown in Figure 2.

Chen and Yang [2004] showed that in western Himalaya and southern Tibet there are two distinct depth intervals of seismicity: 1) upper crustal events above 25 km (in agreement with *Langin et al.* [2003]) and 2) deeper events ~75–100 km deep, near or below the Moho discontinuity. The deep earthquakes are assumed to be in the strong uppermost mantle marking where subduction of oceanic lithosphere ceased tens of millions of years ago [*Chen and Yang*, 2004]. The region of deep (~75–100 km depth) seismicity as discussed by *Chen and Yang* [2004], and confirmed by *Schulte-Pelkum et al.* [2005], obviously would plot beneath the 50 km maximum depth in Plate 2.

Comparing all of the seismicity data with the 50-km-deep MT 800-line+Nepal resistivity section shows that on the northern two-thirds of the profile the seismogenic zone is shallow, above 25 km and above the electrical conductor (Plate 2). Earthquakes are present from the surface to 50 km depth at the southern end of the profile (Plate 2), where the deep conductive zone is absent, and the crust is relatively resistive. A local concentration of earthquakes extending from the surface downward into the conductive zone at ~25 km north of the ITS will be discussed later in concluding Section 7. The main observation in the context of our objectives is that the upper seismogenic zone is above a prominent crustal conductive zone in central and southern Tibet, similar to that observed under the Southern Alps of New Zealand. However, the conductance beneath Tibet is more than an order of magnitude greater reflecting the greater amount of crustal thickening and crustal melting that has occurred beneath this part of the Himalaya.

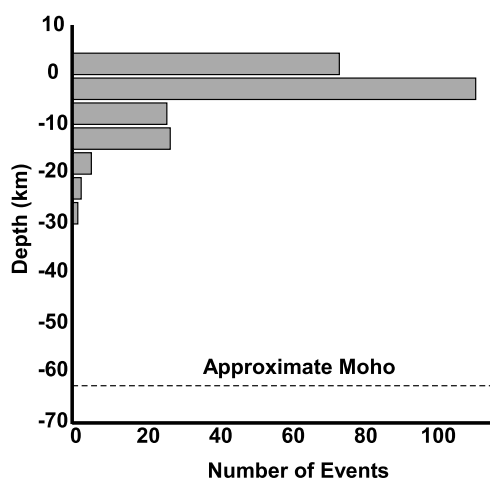


Figure 3. Histogram of depths of earthquakes in 1998–1999 from central Tibet [*Langin et al.*, 2003].

Published MT models for the Himalaya do not require significant resistivity anisotropy as deduced below the Southern Alps, presumably because under the Tibetan Himalaya there is a large melt fraction and less whole-crustal strike-slip shear.

2.3. San Andreas Fault

The 1200-km-long San Andreas fault in California, USA forms the boundary between the North American and Pacific plates (Figure 4). The central California portion of the fault zone is transpressive [Chery *et al.*, 2001], the transpression existing for the last ~ 8 Ma of the 15 Ma old fault system [Atwater and Stock, 1998].

The Parkfield segment of the San Andreas fault, the subject of intense and ongoing research for decades, is located in a transition between a creeping portion of the fault to the northwest and a locked section to the southeast. Long-term strike-slip motion in the Parkfield segment (~35 mm/year) is mainly concentrated on the fault itself along a direction of ~N42°W with only a small (~3 mm/yr) convergent component [Argus and Gordon, 2001]. The Parkfield segment is also where the SAFOD drilling site (<http://www.earthscope.org/safod/index.shtml>) is located (Figure 4) and where a M=6.0, 7.8-km-deep earthquake occurred on September 28, 2004. Aftershocks from this event extended for over 30 km along the fault trace (Figure 4) with all hypocentral depths above 15 km [Thurber *et al.*, 2006]. The SAFOD drilling

program reached its phase 2 objective in the summer of 2005 when the deviated drill hole intersected an active section of the San Andreas fault (Plate 3) at a vertical depth of ~3 km.

There have been a series of papers describing the MT studies in the central portion of the San Andreas fault in California ranging from the creeping segment in the north near Hollister [Bedrosian *et al.*, 2002], to the locked section in the south in the Carrizo Plain [Mackie *et al.*, 1997; Unsworth *et al.*, 1999]. MT results from the Parkfield-SAFOD area in the transitional segment of the fault are numerous [Unsworth *et al.*, 1999; Park and Roberts, 2003; Unsworth and Bedrosian, 2004a, 2004b; Ritter *et al.* 2005; and Becken *et al.*, 2006].

Although the MT data collected in the 1990s across the San Andreas fault were of unprecedented horizontal resolution for that time with site spacings of 100 m near the fault, the maximum depth of resolution was less than 10 km. This was because the profile lengths were short (e.g., <25-km-long for MT line 1 investigated by Unsworth and Bedrosian [2004a]; Figure 4) and the sounding periods were less than 1000 s. In their study of the Parkfield region Unsworth and Bedrosian [2004a, 2004b] performed a series of hypotheses tests using constrained inversions to evaluate the uniqueness of their models. For example, they concluded that the shallow fault zone conductor centered near the surface trace of the fault (SAF in Plate 3) possibly extends deeper than the 2 km they modeled. The very low resistivity (<2 ohm-m) in this zone is thought to be due primarily to saline fluids filling fractures with an overall porosity estimated using Archie's law of 8–30% [Unsworth *et al.*, 1997; Unsworth and Bedrosian, 2004a]. Park and Roberts [2003] suggested that thicker than expected, fluid-filled, conductive sedimentary rocks in the Parkfield syncline immediately (<1 km) east of the fault explains this shallow fault zone conductor. Unsworth and Bedrosian [2004a] cautioned that such shallow fluids in the Parkfield area may not be involved in the earthquake cycle. However, a small mantle component in the fluids sampled from groundwaters and faults adjacent to the San Andreas fault [Kennedy *et al.*, 1997] and in the SAFOD drill hole [Thordsen *et al.*, 2005], possibly associated with upwelling mantle [Sass *et al.* 1997; Jove and Coleman, 1998], provides evidence that there is a connection between the shallow and deeper aseismic crust.

Synthetic inversions of hypothesized structures extending to 40 km below the San Andreas fault by Unsworth and Bedrosian [2004b] concluded that lower crustal structure could be determined under “favorable conditions.” Even so, a model containing a conductive, 5-km-wide vertical extension of the fault into the lower crust was imaged incorrectly as much wider at depth than in the model.

In the spring of 2005 Becken *et al.* [2006] recorded 45 combined long-period/broad-band MT soundings over a 50 by

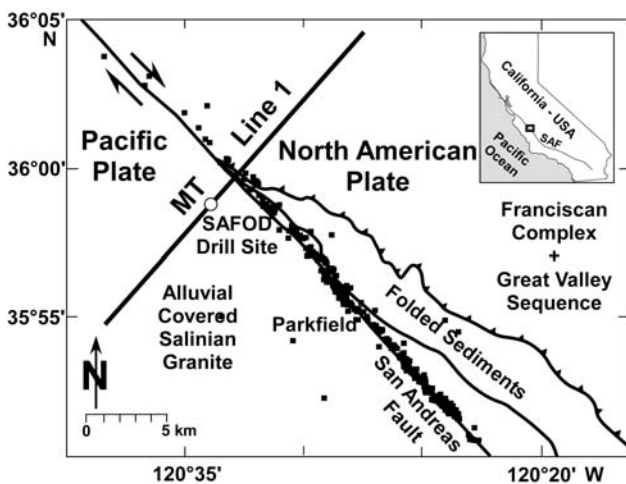


Figure 4. Location map of MT Line 1 in Parkfield, California vicinity of the San Andreas fault [modified from Unsworth and Bedrosian, 2004a]. Surface location of the San Andreas Fault Observatory at Depth (SAFOD) drill site is shown approximately 2 km from the fault. Epicenter locations are of M>2 aftershocks from the 2004 M=6.0 Parkfield earthquake [Thurber *et al.*, 2006].

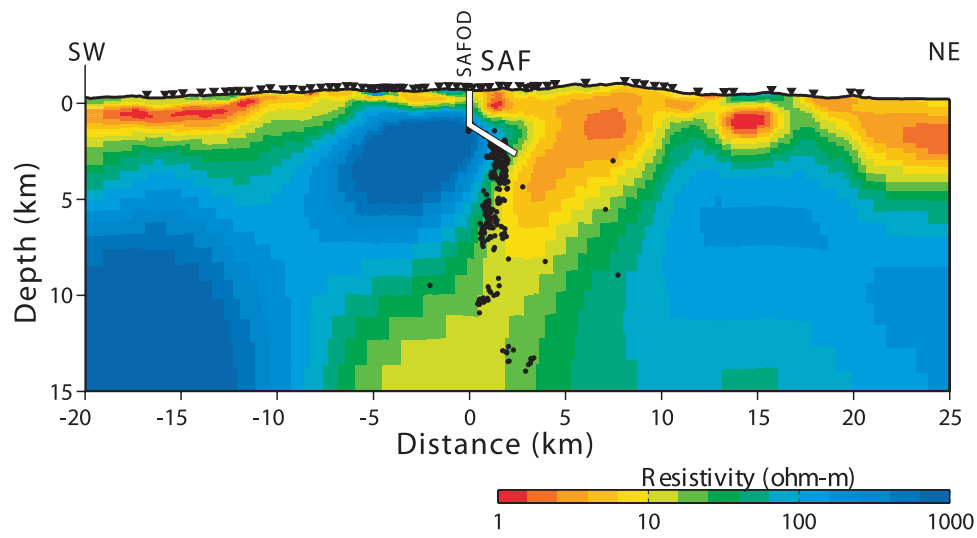


Plate 3. Electrical resistivity model for 2005 MT line from *Becken et al.* [2006; in press, 2007] in the Parkfield-SAFOD area of the San Andreas fault. Inverted triangles are 66 locations of MT sites used in the inversion. Black dots are aftershock hypocenters [*Thurber et al.*, 2006] within ± 3 km of the MT line after projection along fault strike onto the plane of the MT profile.

50 km² area centered on Parkfield. They also collected 41 additional measurements along a previous 45-km-long seismic profile [Hole *et al.*, 2006]. Modeling results of Becken *et al.* [in press] are presented for the upper 15 km in Plate 3 where the upper 6 km of the resistivity profile closely agrees with the shallow section presented by Unsworth and Bedrosian [2004a, 2004b]. The prominent near-surface conductive zone within 10 km east of the fault (previously designated as the Eastern conductor by Unsworth and Bedrosian [2004a]) is thought to be caused by over-pressured fluid within the Franciscan complex and Great Valley sequence (Figure 4). A sub-vertical, ~10-km-wide corridor of high conductivity extends downward from the Eastern conductor through the entire brittle section of the crust where it links with the active seismic zone at a depth of ~5–15 km (Plate 3). Below the 15 km depth section shown in Plate 3 the conductive corridor penetrates vertically along the downward projection of the San Andreas fault through the underlying non-seismic (ductile) crust (15–25 km depth) [Becken *et al.*, 2006, in press]. Becken *et al.* [2006] hypothesized that this deep-reaching conductive anomaly marks a major pathway for deep crust or mantle fluids since it penetrates the entire ~25-km-thick crust.

The deep conductance presented by Becken *et al.* [2006, in press] integrated from 10 to 25 km depth has a maximum conductance of 1500 S and is greater than ~750 S within a zone ~5 km either side of the region of maximum conductance. The high conductance value of 1500 S in the ductile crust beneath the Parkfield segment of the San Andreas fault is intermediate between the high values in the Himalaya (~20,000 S) and New Zealand (~500 S). The lack of a clear depth to the top of the ~10-km-wide conductive zone in the ductile crust beneath the San Andreas fault means that the resistivity pattern is distinctly different than those at the other two continental plate boundaries (Plates 1 and 2). It is nearly centered on the downward projected surface trace of the fault and connects upward through the brittle crust sub-vertically where it is offset east of the surface trace. In New Zealand and the Himalaya the conductive zones in the ductile crust have sharply defined upper boundaries, are laterally extensive, and are situated down dip of the surface expression of the main faults that accommodate convergence. One explanation of the difference may relate to the low convergence rate across the Parkfield portion of the San Andreas fault (~3 mm/yr) compared to the Himalaya (15–20 mm/yr) and New Zealand (~10 mm/yr). In addition, since there is virtually no dip slip along the Parkfield segment of the San Andreas fault there is little opportunity for fluid production though crustal thickening and metamorphism.

Where the San Andreas fault zone is narrow, seismicity is localized (Figure 4 and Plate 3) within the near-vertical extensions of the fault itself, slightly offset from its surface

trace, or along near-downward projections of steeping dipping auxiliary faults [Thurber *et al.*, 1997, 2006; Bedrosian *et al.*, 2004]. Whether the fault is locked, creeping, or has recently ruptured, more than 99% of modern and historic earthquakes occur in the upper 15 km for the San Andreas system as has been known for some time [Brace and Byerlee, 1970]. Plate 3 includes aftershock hypocenters from the 2004, M=6.0 Parkfield earthquake [Thurber *et al.*, 2006] that occurred within ±3 km of the Becken *et al.* [2006, in press] MT profile. This profile extends from both ends of MT Line 1 in Figure 4 where the epicenters of M>2 earthquakes from the 2004 event are plotted.

There is scant evidence of the exact nature of the ductile crust beneath the San Andreas fault. Unsworth and Bedrosian [2004b], citing the work of Anderson *et al.* [1983] on exhumed fault zones, suggest a narrow, vertical mylonite zone where fluid and shearing would enhance the electrical conductivity not unlike what we have proposed beneath the Southern Alps in New Zealand.

3. DEEP FLUIDIZED ZONES

Source regions of fluid release must feed each of the deep conductive zones. In the case of the Southern Alps the fluid is thought to originate from a thickened crust [Koons *et al.*, 1998; Vry *et al.*, 2001; Wannamaker *et al.*, 2002; Upton *et al.*, 2003; Upton and Koons, this volume] and in the Himalaya from within thickened underthrust Indian lithosphere [Makovsky and Klemperer, 1999; DeCelles *et al.*, 2002; Klemperer, 2006]. Below the San Andreas fault, fluid is hypothesized to be produced in the deep crust [Rice, 1992; Pili *et al.*, 1998; Gratier *et al.*, 2003] and from an upwelling mantle [Zandt and Carrigan, 1993; Kennedy *et al.*, 1997; Sass *et al.*, 1997; Jove and Coleman, 1998; Thordsen *et al.*, 2005]. In New Zealand and the Himalaya the conductive zones are distinct with upper bounds clearly beneath the seismogenic crust. In the ductile regime below the San Andreas fault, a sub-vertical conductive pattern is centered on the fault and it has no distinct top. To explore these relations we consult the extensive literature on the occurrence and fate of deep metamorphic fluids [e.g., Ferry, 1994; Connolly, 1997; Manning and Ingebritsen, 1999] and the formation of fluid reservoirs below and at the brittle-ductile transition [Bailey, 1994; Connolly and Podladchikov, 2004; Hobbs *et al.*, 2004; Cox, 2005].

Bailey [1994] described a sealing mechanism in the mid-crust due to the formation of immiscible CO₂-H₂O mixtures below which rising fluids could pond. He argued that the process would operate best just above the brittle-ductile transition and that such sealing would not be permanent below the transition. Hydraulic fracturing, induced by the

continued arrival of high-pressure fluids from below, would be expected to be horizontal (perpendicular to the minimum principal stress which is vertical) in stable or compressional tectonic regimes. This would result in very thin fluid reservoirs compared to their horizontal extent as described earlier by Bailey [1990].

Connolly [1997] extended the work of Connolly and Thompson [1989] and Thompson and Connolly [1990] to study the migration of devolatilization-generated fluids by numerical simulations of heating at various rates at 25 km crustal depth. The accompanying metamorphic reactions released water exceeding 1% by weight in some cases. The main finding of Connolly's simulations was that metamorphic dehydration processes perturb the steady state hydrologic regime enough to produce shock waves of anomalous fluid pressure, porosity, and fluid flux. He found that compaction caused by the difference between the confining pressure and vertical fluid pressure gradients generated positive fluid pressure above the reaction (fluid release) front. This launched an upward propagating porosity wave leaving a connected pore network in its wake. Hydrofracture is possible at shallower depths as the upward strengthening of the crust slows the porosity waves and increases their wavelength and pressure amplitude. Upward slowing of porosity waves also allows newly launched waves to interact with earlier ones [Connolly, 1997]. As this occurs, the porosity of the wave continues to increase as fluid is transferred from deeper waves. This process leads to mechanical stability with a positive feedback system favoring the formation of high-porosity so-called "water sills" [Fyfe *et al.*, 1978; Connolly, 1997]. Such features have low shear strength so they would be unstable under deviatoric stress. The model calculations showed that water sills can form in rheologically continuous, upward strengthening media but the time required is long (>50 Myr). However, a crustal strength discontinuity greatly accelerates their formation. This means that a relatively impermeable or strong lithologic barrier below the brittle-ductile transition is required to arrest upward fluid migration in young, active tectonic regimes. For example, in a simulation presented by Connolly [1997], a stronger layer (by a factor of 20 times) at 17 km depth was enough to stall an upward propagating porosity wave within the time scale of 5–10 Myr after generation of the reaction front at 20 km depth.

Connolly and Podladchikov [2004] proposed another mechanism to trap fluid in the ductile crust in compressional tectonic settings. They showed that in such environments the absence of a vertical hydraulic gradient below the brittle-ductile transition produces a zone of fluid stagnation (Figure 5). This occurs because the buoyancy forces acting on a fluid are balanced by the vertical stress gradient in the rock [Connolly and Podladchikov, 2004]. This not only explains how upward migrating

fluids are arrested but also how fluids from above will flow downward into a reservoir below the brittle-ductile transition. Thus, wherever a stagnation zone is formed in the ductile crust there is a zone of negative hydraulic potential gradient above that drives fluid flow downward and a positive gradient below that drives flow upward (Figure 5). The vertical potential gradient in between is zero so the fluid is trapped. Connolly and Podladchikov [2004] called this tectonically induced neutral buoyancy because its formation depends on differential stress that develops in response to horizontal compressive stress.

Using ranges of estimated parameters, the authors calculated possible stagnant zones for aqueous fluid up to 12 km thick and 20 km below the brittle-ductile transition. The

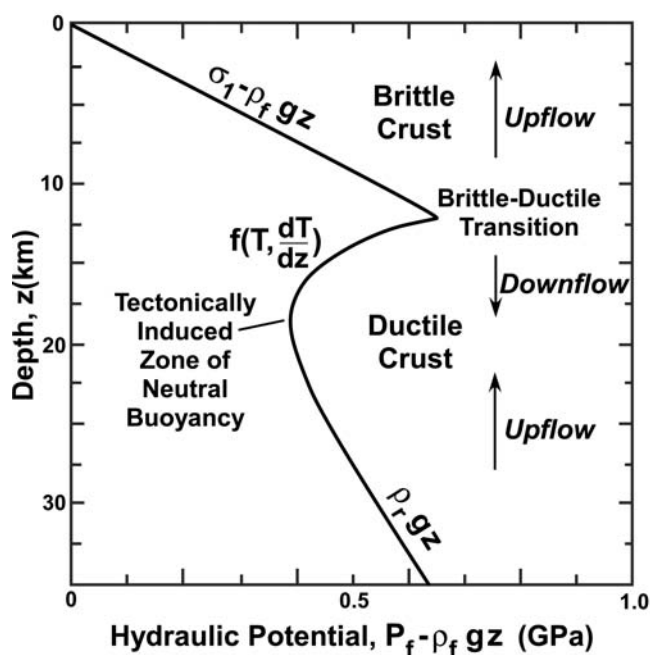


Figure 5. Profile of hydraulic potential versus depth for a 2-D pure shear, compressional model of the crust [modified after Connolly and Podladchikov, 2004]. Byerlee's law is assumed for the brittle crust using fluid density ρ_f . A differential stress ($\sigma_1 - \sigma_3$) term included in the fluid pressure, P_f calculation results in suprahydrostatic hydraulic potential, $\sigma_1 - \rho_f g z$ where g is the gravitational acceleration. Thermally activated ductile behavior below the brittle-ductile transition decays toward lithostatic conditions at depth for rock density ρ_r . A region of tectonically induced neutral buoyancy is developed below the brittle-ductile transition where the vertical hydraulic gradient is zero and water flows from above and below into a zone of fluid stagnation. This would result in a conductive zone in the ductile crust. Specific values of GPa versus depth were calculated using estimated crustal parameters including temperature, T and its vertical gradient [Connolly and Podladchikov, 2004].

concept of tectonically induced neutral buoyancy expands on the “Swiss cheese” model (Figure 6) of the crust [Connolly and Podladchikov, 2004] where fluid circulates freely in the brittle crust and is allowed only in self-propagating, isolated domains of various geometries in the ductile crust (Figure 6). Fluid flow in these domains is sensitive to tectonic forcing and can be accomplished through an individual fracture, a network of fluid-filled fractures, or via grain-edge porosity (discussed in Section 4). In either case, the vertical pressure gradient, $\partial P_f / \partial z$ in a spherical domain has the same mean stress gradient as the surrounding rocks. The gradient approaches the vertical gradient of the horizontal, σ_1 and vertical component, σ_3 of the far-field stress for vertically and horizontally elongate domains, respectively (Figure 6). Connolly and Podladchikov [2004] described the result that the brittle-ductile transition would act as a barrier to upward propagating domains (in the form of porosity waves as discussed above) with spherical or vertical geometries. However, far field compressive stress would promote a dynamic evolution of these geometries to spread laterally during upward ascent resulting in coalesced, quasi-static fluid bearing horizons. It is important to note that the fluid accumulation mechanism in the ductile crust described by Connolly and Podladchikov [2004] is valid for any fluid, including partial melt.

The work of Hobbs *et al.* [2004] independently confirmed Connolly and Podladchikov’s prediction of regions of stag-

nant fluid flow in the ductile portion of the crust. In fact, where the geothermal gradient is high, multiple zones are predicted. Multiple zones are also predicted by Connolly and Podladchikov [2004] because numerous porosity waves would occur during episodic or continuous, deep metamorphic reactions. Hobbs *et al.* [2004] numerical models included a weak zone dipping at 45° in the brittle crust to simulate a fault extending to the brittle-ductile transition (Plate 4a). The 2-D numerical modeling assumed a crust initially saturated with fluid with pore pressure sufficient to hold pore space open without causing failure. The crust was then shortened horizontally at a given strain rate and patterns of dilatancy were computed. For example, Plate 4b shows the instantaneous volumetric strain rate where there was 1.5% shortening. Here, dilatant zones represent zones of increased porosity and, therefore, excess fluid. They are developed as near-horizontal, tabular features (Plate 4b) at the brittle-ductile transition and above along the hanging wall of the numerically inserted fault (Plate 4a) and *en echelon* to it along a diffuse backthrust shear zone. These features are the direct result of strain partitioning that produces a plastic wedge of material involving the entire brittle crust. This wedge shape is very similar to the conductive pattern below South Island of New Zealand (Plate 1) except for one major difference: the bottom of the conductive feature in New Zealand is not at the brittle-ductile transition, it is well below it in the ductile crust. Hobbs *et al.* [2004]

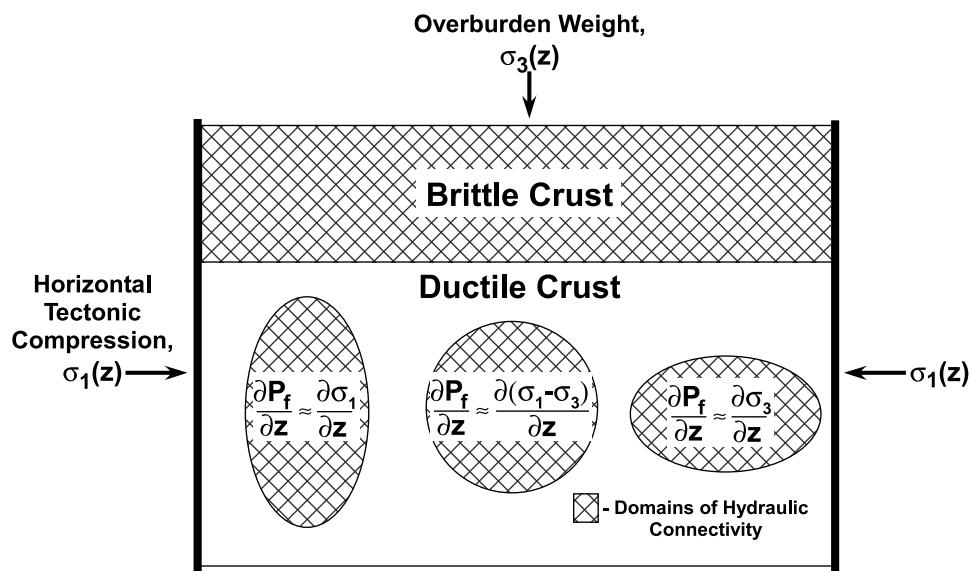


Figure 6. “Swiss cheese” model of the crust [modified after Connolly and Podladchikov, 2004] during horizontal compression, σ_1 in which fluid circulates freely in the brittle crust but occurs in isolated fluid-rich domains in the ductile crust. The shape of the isolated domains governs whether the vertical pressure gradient is dominated by the far field compressive stress, σ_1 (in vertically elongated domains), the mean stress ($\sigma_1 - \sigma_3$) (in spherical domains), or the vertical overburden stress, σ_3 (in horizontally elongate domains).

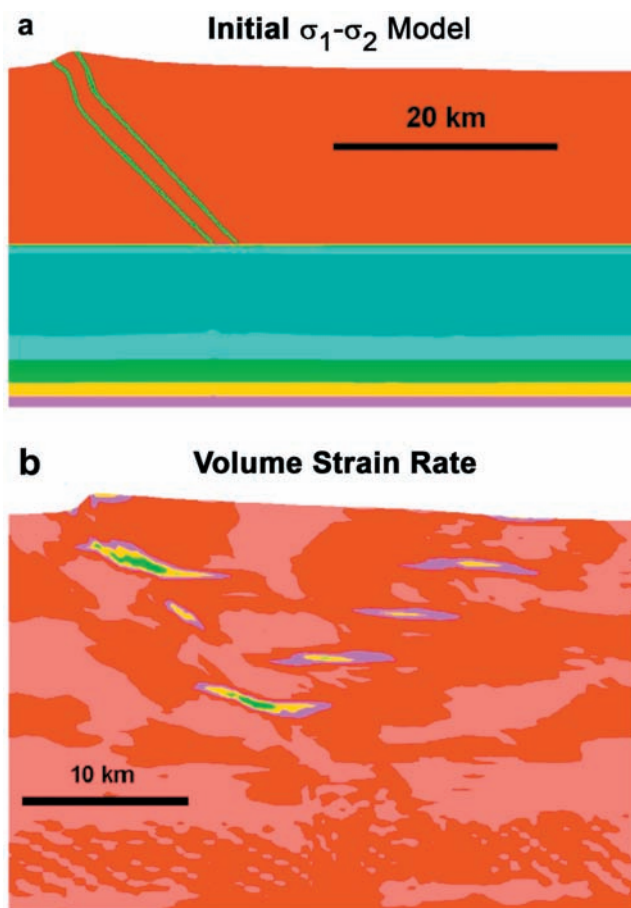


Plate 4. (a) Initial geometry of 2-D numerical model from *Hobbs et al.* [2004] shown by plot of $(\sigma_1 - \sigma_2)$ using a geothermal gradient of 20°C/km. Inserted fault is outlined in green. Red is plastic (brittle) portion of the crust corresponding to 0–500 MPa. Below is viscous (ductile) crust. Darkest blue is maximum $(\sigma_1 - \sigma_2)$ corresponding to 3 GPa and greater. Contour interval is 500 MPa. (b) Plot of instantaneous volumetric strain rate using geothermal gradient of 40°C/km. Dark green: $3.2 \times 10^{-11}/s$; yellow: $2.4 \times 10^{-11}/s$, purple: $1.6 \times 10^{-11}/s$, contour interval: $0.8 \times 10^{-11}/s$. Total shortening is 1.5%; from *Hobbs et al.* [2004].

numerical modeling did not include the necessary coupling between deformation and induced porosity production in the viscous (ductile) portion of the crust so zones of increased porosity were not modeled there as they were in the plastic (brittle) upper crust. Nevertheless, the result from *Hobbs et al.* [2004] illustrates the pattern of fluidized zones resulting from hydrofracturing in compressional settings and serves to encourage numerical modeling aimed at studying porosity evolution and its consequences in the ductile crust.

Hobbs et al. [2004] pointed out that there would be different mineral alteration patterns in fluid zones formed in the brittle crust compared to the stagnation zones in the ductile crust. This is because fluid flow above a fluid-stagnant zone is in the same direction as the geothermal gradient (downward) and it's in the opposite direction (upward) in the lower section. In the brittle crust, flow is opposite to the geothermal gradient and fluids ascend (Figure 5). The results would be asymmetric mineral alteration patterns for fluid stagnation zones originating in the lower ductile, crust and homogeneous alteration patterns in the upper crust, features that may be observable in exhumed midcrustal terranes.

The above considerations lead us to expect that fluid generated by deep episodic or near steady state metamorphic processes would be propagated upward and ponded beneath strong lithologic contrasts present below the brittle-ductile transition. Time scales required for the formation of such fluid-rich zones beneath inhomogeneities would be only ~5–10 Myr compared to >50 Myr in rheologically homogeneous, upward strengthening ductile crust. This process would occur independent of the tectonic setting [compressional or extensional; *Connolly and Podladchikov*, 2004]. Fluid-bearing horizons also would occur below the brittle-ductile transition in regions of neutral buoyancy in compressional environments. In either case the fluid is expected to spread horizontally. Water sills can be stable for long times (tens of Myr) even by geologic standards and even longer in compressional environments [*Thompson and Connolly*, 1990]. However, their low shear strength (due to high fluid content) would make them unstable under deviatoric stress [*Connolly*, 1997].

4. INTERCONNECTIVITY OF FLUIDIZED ZONES

If the proportion of aqueous fluid in the ductile crust is <1%, it must be interconnected to have resistivities lower than a few 100 ohm-m. This requires either a fluid-filled fracture network, grain-edge interconnection, or both (so-called dual porosity). Either possibility is allowed in the mechanisms discussed above [*Connolly and Podladchikov*, 2004]. Experimental work has shown that fracture networks with high crack connectivity and permeability can form in

ductile regimes at low strain rates provided the fluid pressure is elevated compared to the vertical stress [*Cox*, 2005]. Since the state of stress in a material is expressed by a second-order tensor, there are always three orthogonal vectors that define the principal stress directions. In compressional tectonics the maximum principal stress, σ_1 is horizontal and the least principal stress, σ_3 is vertical (Figure 6).

4.1. Fracture Connectivity

In the presence of fluids, pure extensional fractures are initiated perpendicular to the minimum principal stress (σ_3) if the fluid pressure equals or exceeds the sum of σ_3 and the tensile strength of the rock [*Cox*, 2005]. Stress on a fracture can be decomposed into a component in a direction parallel to the fracture plane (shear stress) and one perpendicular to it (normal stress). The effects of these components are highly coupled in the sense that deformation caused by a change in one is dependent on the magnitude of the other [*National Research Council*, 1996]. If an extensional fracture is already present but closed, the fluid pressure to reopen it is equal to the normal, i.e., compressive, stress across the fracture. For fractures to remain open, and therefore interconnected, the effective stress in the rock, generally taken as the normal stress on the fracture minus the fluid pressure therein [e.g., *National Research Council*, 1996] must remain positive. If the effective stress is zero the fractures close. The rock will undergo extensional hydrofracture if the effective stress is negative and satisfies a yield condition.

Because extensional cracks form perpendicular to the minimum compressive stress, they would be horizontal in compressive environments. However, shear fractures and hybrid extensional-shear fractures form at oblique angles to σ_3 , typically between $\pm 20^\circ$ to 35° and 0° to $\pm 25^\circ$ to σ_1 , respectively [*Cox*, 2005]. Pure extension fractures open perpendicular to the fracture wall, whereas, displacement in shear fractures is parallel to the fracture plane. Hybrid fractures are defined where there is displacement both parallel and perpendicular to the fracture plane. Pure extensional failure occurs at relatively small stress differences ($\sigma_1 - \sigma_3$) coupled with high fluid pressure. In contrast, if the stress difference is increased, shear fracture can result under conditions of low fluid pressure [*Cox*, 2005].

Maintenance of fracture porosity during interseismic periods is a complex function of space and time. Sustained elevated fracture permeability in the ductile crust usually requires continued deformation, high fluid pressure, and/or permeability enhancing reactions [*Cox*, 2005]. If such conditions are not met, fluids can become isolated and pressurized locally because cracks seal during episodes of low fluid pressure gradients [*Byerlee*, 1990].

4.2. Grain-Edge Connectivity

For grain-edge (intergranular) porosity, recrystallization before and during fluid ascent can lead to the creation of connected pore networks (permeability) that can be maintained over geologically significant times [Brenan, 1991]. Under conditions of both mechanical and chemical equilibrium, the distribution of intergranular fluid is one that minimizes the total interfacial energy of the system, leading to “textural equilibrium” [Watson *et al.*, 1990; Spear, 1993; Holness, 1997]. The interfacial energy depends on the mineral and fluid phases, the mineral major- and minor trace-element composition, temperature, pressure, and crystal orientations [Watson *et al.*, 1990]. Knowledge of the interfacial energy is usually unknown or is too imprecise to be useful [Brenan, 1991]. However, at textural equilibrium there are well-defined angular relationships between the fluid and grain boundaries that define the wetting characteristics. In a monomineralic, texturally equilibrated, isotropic material undergoing recrystallization, an angle, called the wetting angle or dihedral angle, θ determines the 3-D connectivity of the fluid-filled pores. The dihedral angle is the angle of intersection where mineral grains make contact with the fluid [Figure 7a; Brenan, 1991]. For low porosity rocks (< 1%), grain-edge tubes remain connected if $\theta \leq 60^\circ$; the tubes pinch off and the fluid is isolated at grain-edge intersections if $\theta > 60^\circ$ [Figure 7b; Watson *et al.*, 1990]. A stable, thick fluid would completely wet all grain boundaries at a dihedral angle of 0° . At $\theta = 180^\circ$ the fluid is isolated in spherical cavities (Figure 7).

The majority of the experimental determinations of equilibrium fluid topologies have been obtained from monomineralic grain aggregates, but recent studies have demonstrated greatly increased pore fluid connectivity in systems with traces of other mineral phases [e.g., Holness, 1995; 1998; Yoshino *et al.*, 2002]. Earlier work by Watson and Brenan [1987] on aqueous fluids with monomineralic aggregates and synthetic mafic rocks (primarily quartz and dunite, respectively) discovered θ just below 60° for quartz (implying interconnectivity) but high dihedral angles for the mafic rocks. Salts (NaCl, KCl) added to the aqueous fluid significantly lowered θ (to $\sim 40^\circ$) in the quartz-fluid system but had no effect on the high wetting angles in dunite (implying isolated pores). The addition of CO_2 increased θ to $> 60^\circ$ in all cases. Therefore, Watson and Brenan [1987] concluded that aqueous fluids in the ductile portion of the crust are likely to be interconnected especially if the water is saline and CO_2 -poor, but aqueous fluid in the ultramafic uppermost mantle would exist in isolated pores.

For equilibrium wetting to occur, the rate at which equilibrium is reached must be faster than the strain rate of ductile deformation or of any other rate limited nonequilibrium processes [Brenan, 1991]. This means that the rate of equilibration is about equal to the rate of change of porosity so if fluid production (or loss) is too rapid, textural equilibrium is not achieved [Holness and Siklos, 2000]. Tullis *et al.* [1996] reported on laboratory experiments where the increased deformation of “water-added” feldspar aggregates at high temperature and pressure mimicked that of aggregates containing a fluid with a dihedral angle of 0° (total grain

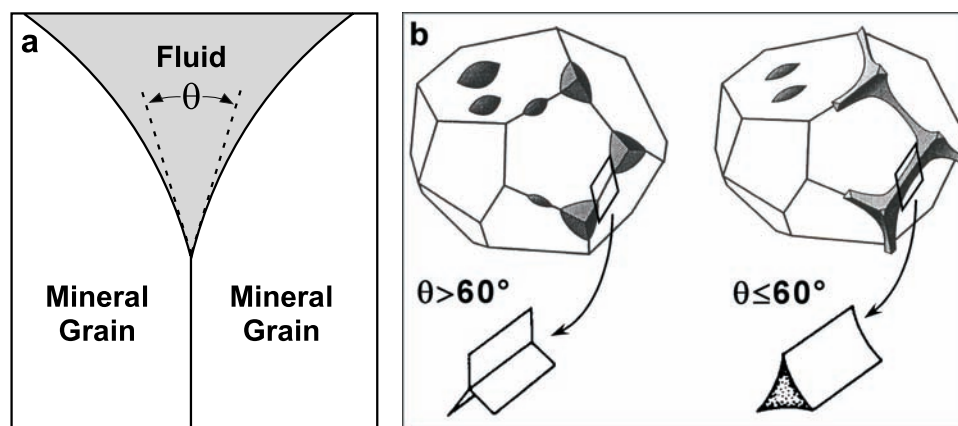


Figure 7. (a) Cross section through a fluid-filled grain-edge channel at the intersection of two minerals grains and the definition of the wetting or dihedral angle, θ ; modified from Brenan [1991]. (b) 3-D fluid distribution along a mineral grain where fluid occurs in isolated pores, $\theta > 60^\circ$ and where there is interconnectivity, $\theta \leq 60^\circ$; modified from Watson *et al.* [1990].

wetting). The authors pointed out that this result is consistent with enhanced fluid permeability and material transport along fluid-filled grain boundaries in ductile shear zones in the mid-crust.

5. EARTHQUAKES AND FLUIDS IN THE DUCTILE CRUST

The question we explore now is in what ways fluidized zones at or below the brittle-ductile transition can play a role in the earthquake cycle. There seems to be no question that large earthquake ruptures in the brittle crust can propagate downward into the ductile region thereby releasing fluid trapped below the brittle-ductile transition [e.g., *Cox*, 2005]. Draining of these fluid reservoirs requires them to have enhanced permeability pathways as developed by deformation and/or high fluid pressure in ductile shear zones. Fluid-triggered aftershocks [e.g., *Nur and Booker*, 1972] occur in the brittle crust after the main shock of an earthquake due to upward migrating fluid-pressure pulses (*Sibson's* [1992] fault-valve concept), and from coseismic stress transfer [*Cox*, 2005]. A more uncertain scenario is how earthquake rupture in the brittle crust is initiated by permeable, overpressured fluidized zones in the ductile crust. Addressing this possibility requires reviewing the basics of how earthquake rupture occurs.

Failure initiating an earthquake occurs when the tectonic shear stress on the fault exceeds some critical value. The process leading to localized unstable stick-slip, or earthquake nucleation, can be expressed as a constitutive relation that depends on several factors including the slip rate, temperature, pressure, rock composition, and fluid state. When the relationship exhibits rate-weakening, rather than rate-strengthening, the localized deformation causes friction to decrease resulting in velocity weakening. Such a condition allows earthquake nucleation provided that a patch on the fault greater than some critical dimension becomes unstable and slips [*National Research Council*, 2003; *Rice and Cocco*, 2007]. The suggestion that earthquake nucleation can be triggered by fluid processes originating below the actual seismogenic zone is motivated by the spatial relationships between deep conductivity zones and seismicity in New Zealand (Plate 1) and the Himalaya (Plate 2). The idea has been independently bolstered by recent observations of nonvolcanic, episodic tremor and slow slip in the Cascadia subduction zone [*Rogers and Dragert*, 2003] and below the San Andreas fault [*Nadeau and Dolenc*, 2005]. The exact manner by which events tens of kilometers beneath the seismogenic zone connect to earthquakes in the upper seismogenic crust is unknown. However, the prevailing view is that the tremors are generated by processes associated with fluids [*Nadeau and Dolenc*, 2005; *Shelly et al.*, 2006].

Iio and Kobayashi [2002] proposed that seismic failure along an active fault in the upper, brittle crust can be triggered by localized, aseismic motion on a shallow-dipping shear zone in the ductile crust. *Hobbs et al.* [2004] investigated this possibility numerically; however, they concluded that to fully understand the proposal of *Iio and Kobayashi* [2002] requires a better understanding of crustal rheology than is presently available. Two of the questions posed by *Hobbs et al.* [2002] were: 1) what processes can produce the strain softening required to localize deformation in the lower, ductile crust and 2) are there mechanisms in the lower, ductile crust that could generate earthquakes?

Hobbs et al. [2002] cited evidence that localized deformation requires strain softening if the lower crust behaves in a simple viscous manner. Softening can occur in a viscous material via several processes including water-weakening, micro-cracking, and thermal softening. Deformation in a classical power-law, viscous material is always distributed unless there is such softening. *Hobbs et al.* [2002] also pointed out that localization would be ubiquitous for hybrid elasto-viscous-plastic behavior such as a transitional zone between the brittle and ductile portions of the crust. Such a transition zone would allow "ductile fracture" and a proposal that earthquakes could be generated by unstable sliding on the fractures. Velocity weakening and unstable sliding in materials under conditions where ductile behavior normally dominates is considered by *Hobbs et al.* [2002] to be an important mechanism for earthquake generation at midcrustal depths especially if spaces between asperities are filled with overpressured fluid.

Water-weakening would occur in the fluid stagnation zones described by *Connolly and Podladchikov* [2004] and *Hobbs et al.* [2004] if sufficient fluid-filled porosity exists. Combining the upward propagating porosity waves of *Connolly* [1997] with these stagnation zones is one mechanism that would produce such porosity. *Connolly and Podladchikov* [2004] discussed two mechanisms by which fluids in such overpressured zones could be propagated upward 5 to 7 km above the zone of stagnation thus breaching the brittle-ductile transition. According to *Connolly and Podladchikov* [2004] the zone in which fluids accumulate and are trapped may simply thicken upward eventually breaching the brittle-ductile transition releasing fluids into the overlying brittle crust. This process will occur if the fluid, accommodated by ductile deformation, accumulates faster than the ductile compaction rate. Another way to release fluids from the stagnation zone into the brittle crust is to invoke a relaxation of compressive tectonic stresses, thereby, changing the principal stress relations and causing upward propagating hydrofractures [*Connolly and Podladchikov*, 2004]. In either case, the release of fluid will increase fluid pressures in the upper crust and possibly initiate seismic rupture.

Recognizing the uncertain role of the ductile crust in earthquake generation, *Hobbs et al.* [2002] concluded that “there is a wealth of work to be done to understand the coupling between dilation, fluids, and constitutive relations for lower (ductile) crustal rocks and the controls on localization and unstable sliding.” We agree that this remains a field of important future study.

6. DISCUSSION AND CONCLUSIONS

The role of fluids during the entire earthquake cycle may control the processes of fault rupture, propagation, and arrest [*Hickman et al.*, 1995]. We have attempted to answer the question of how the spatial distribution of aqueous fluids at or below the brittle-ductile transition relates to seismicity at three continental plate boundaries in New Zealand, the Himalaya, and along the Parkfield segment of the San Andreas fault. We assumed that MT imaging of conductive zones in these locations is mapping zones of interconnected fluid. Table 1 summarizes our observations.

The seismogenic zones in New Zealand and the Himalaya are distinctly above the midcrustal conductors. The situation is less clear for the Parkfield segment of the San Andreas fault where the most recent MT results show a near-vertical conductor throughout the ductile crust which extends upward to a near-surface conductive zone centered east of the fault. The conductance of the near-vertical feature is intermedi-

ate in magnitude compared to the conductances of the sub-horizontal, low resistivity zones in the ductile crust of the Southern Alps and the Himalaya (Table 1). The Himalaya conductance exceeds that beneath the Southern Alps by more than an order of magnitude (Table 1). The low resistivity of the Himalaya deep conductor it is interpreted to be a thick, partial melt zone with aqueous fluid residing on top. We believe that the best explanation of the conductive zone under the Southern Alps is that of a mylonized, fluid-rich, active, ductile shear zone. The high conductance in the ductile crust beneath the San Andreas fault conductive zone may also mark a ductile shear zone that is vertically oriented as suggested by *Eberhart-Phillips et al.* [1995] and *Unsworth and Bedrosian.* [2004b]. Such interpretations are consistent with the results of *Tullis et al.* [1996] and *Famin and Nakashima* [2004] that microfracture permeability and/or grain-edge wetting is enhanced in active ductile shear zones.

Comparing conductive occurrences with seismicity in the three tectonic settings necessarily requires considering several factors. These include:

1. The compressional Himalaya has the longer history of convergence tectonics (~50 Myr), the width of the orogen (~400 km) and its convergence rate (15–25 mm/yr) are the largest, and the crustal thickening is greatest (>80 km).

2. The transpressional Southern Alps in New Zealand have a compressional history only for the last ~5 Myr with convergence averaging about 10 mm/yr, the width of the central

Table 1. Properties of Seismogenic, Electrically Conductive, and Fluid Zones in the Ductile Crust and Plate Motions at Three Continental Plate Boundaries (see text for sources of information).

	Alpine Fault –Southern Alps, New Zealand	Himalaya, Central and Southern Tibet	San Andreas Fault, California, USA
Depth Extent of Seismogenic Crust	~12 km	~ 25 km	~15 km
Depth to Top of Conductive Zone	~ 20 km	~25–40 km	No Distinct Top; Sub-Vertical Corridor Extends Through Entire Ductile Crust
Conductance of Conductive Zone	50 to 500 S	3000 to >20,000 S	750 to 1500 S
Fluid Content	≤3% Aqueous Fluid	~10% Aqueous Fluid Above Thicker, 5–14% Partial Melt	Uncertain % Aqueous Fluid
Fluid Origin	H ₂ O Released from Prograde Metamorphism in Thickened Crustal Root and Strain-Induced Metamorphism within a Ductile Shear Zone.	Heating of Double Thick Crust. H ₂ O Released from Melting, Prograde Metamorphism, and/or Dehydration of Subducted Indian Crust.	H ₂ O Released from Mantle and Strain-Induced Metamorphism within a Ductile Shear Zone.
Relative Plate Motion	Strike Slip: 35 mm/yr Convergence: 10 mm/yr	Convergence: 15–20 mm/yr	Strike Slip: 35 mm/yr Convergence: 3 mm/yr

portion of the orogen is ~100 km, and the maximum crustal thickness is ~45 km [Schervath *et al.*, 2003; van Avendonk *et al.*, 2004].

3. In the central segment of the ~8 Myr old San Andreas fault there is very little convergence (~3 mm/yr) and, therefore, limited crustal thickening; the strike slip component of strain is large (~35 mm/yr), about the same as along the Alpine fault in New Zealand.

Given the above similarities and differences we now comment on their relevance:

1. High convergence in New Zealand and the Himalaya produces uplift, mountain building, crustal thickening, and the deep release of aqueous fluid through prograde metamorphism in a crustal root. Additionally, greater crustal thickening in the Himalaya has promoted partial melting and further release of aqueous fluid. Release of aqueous fluid through prograde metamorphism in a thickened crustal root would not occur below the low relief Parkfield area of the San Andreas fault.

2. Laterally extensive fluid reservoirs formed by the arrest of upward propagating porosity waves at permeability or strength discontinuities, or regions of neutral buoyancy, are favored in compressional settings [Connolly, 1997]. But low convergence rates, such as the 3 mm/yr across the San Andreas study area, may not allow their formation. The only place along the San Andreas fault where significantly higher compression occurs is in the Transverse Ranges where the convergence is 7.7 to 10.6 mm/yr [Godfrey *et al.*, 2002].

3. A sub-vertical conductive zone occurs in the ductile crust beneath the San Andreas fault in the Parkfield-SAFOD area and appears to continue uninterrupted to the surface. This may reflect insufficient permeability or lithologic heterogeneity needed to arrest and pond upward migrating fluid in such a young tectonic setting. For example, the time required to form water sills in rheologically homogeneous circumstances is estimated to exceed 50 Myr. However, in the simulations run by Connolly [1997], formation times decreased to ~5 Myr when there is an order of magnitude increase in rock strength. Therefore, with a sufficiently large strength change in the lower crust in the Southern Alps a water sill could have formed in the last ~5 Myr. This would have facilitated water-weakening and development, or increased development, of a near-horizontal, mylonized, ductile shear zone.

4. A horizontally limited conductor under the San Andreas fault may be a near-vertical, ductile shear zone below the brittle seismogenic zone. Shear strain strongly affects fluid interconnection enhancing electrical conductivity even though the amount of fluid may be small (<1%). Also, strike-slip deformation leads to the creation of long backbone shears

and increases the proportion of backbone to isolated, fluid-bearing elements [Cox, 2005].

5. Greater fluid interconnection and reduction of resistivity in the strike-slip direction is expected in highly transpressional orogens like the New Zealand Southern Alps [Wannamaker, 2005]. This would explain the strong resistivity anisotropy inferred there. The crustal conductor below the San Andreas fault may turn out to be anisotropic with greater conductivity along strike due to shearing. That the Himalaya exhibit relatively limited electrical anisotropy despite the pronounced high conductivity is attributed, in part, to it being a more purely compressional regime.

6. We note that there is no MT detection of through-going pathways from the surface to the deep conductor found in the Himalaya results of Unsworth *et al.* [2005] as there are in New Zealand and along the San Andreas fault. However, new MT modeling by Arora *et al.* [2007] along the NW Himalaya line (Figure 2) reveals that the ITS appears to mark a low resistivity connection to the deep conductor. This may relate to crustal extension in western Himalaya in the area [Zhang *et al.*, 2004]. The deep conductor in northwest Himalaya is also much less conductive (by a factor of 2 to 3) compared to that in Tibet possibly because there is no evidence there of continental magmatism [Arora *et al.*, 2007].

7. The occurrence of earthquakes crossing the upper boundary of the conductive layer in the Himalaya (at about 25 km north of the ITS in Plate 2) may have been initiated by fluid propagation downward along deep penetrating ruptures or by catastrophic upward breaching of the brittle-ductile transition by high pressure pore fluid as we have suggested. However, inaccuracies in focal depth estimates and the projection of hypocenters ~100 km from the MT profile (Figure 2 and Plate 2) make such assertions speculative.

Localized deformation in the ductile crust is possible where strain softening occurs. Since water-weakening is one mechanism to do this, the fluidized zones detected by MT soundings may be imaging zones of localized ductile shear as we surmise in New Zealand. Aseismic slip in these zones may couple directly upward along deeply penetrating faults or stress loading may be propagated above into the brittle crust. Rapid fluid expulsion could perturb the stress state enough to trigger earthquakes in the seismogenic crust. Fluid concentrations trapped under the seismogenic zones beneath the Southern Alps and the Himalaya are likely to be overpressured through continuous generation of fluids from below which upon release could initiate earthquakes. MT results from the Parkfield area of the San Andreas fault suggest that fluids are untapped and continuously raising which may facilitate lesser magnitude but more frequent seismicity compared to the Southern Alps and the Himalaya. This perhaps explains the short recurrence interval of tens of years

for moderate earthquakes in the Parkfield area of the San Andreas fault [*Bakum and Lindh*, 1985].

Our study of three continental plate boundaries, and the appropriate literature, establishes experimental and numerical evidence for the occurrence of trapped fluidized zones in the ductile crust. Detectability of deep, interconnected fluidized zones by MT is unmatched below seismogenic depths, therefore, MT promises a unique contribution to understanding the earthquake cycle. MT images of the crust are providing well-constrained depths to fluid concentrations that may turn out to be tied to earthquake rupture above. We call for more high quality MT surveys in a variety of tectonic settings and laboratory conductivity measurements of continental rocks at midcrustal, fluid bearing conditions while undergoing strain. Ultimately, temporal changes in the measured MT response of large fluidized regions in the ductile crust and their extensions upward into the active seismogenic crust combined with continuously recorded GPS surface distortion data, tilt measurements, and tremor activity could reveal measurable earthquake precursors.

Acknowledgments. The MT program in New Zealand was supported by the U. S. National Science Foundation (NSF) grants EAR98530 and EAR97-25883 (Continental Dynamics) and by the New Zealand Foundation for Research Science and Technology. Kilb's contributions were supported by NSF award EAR 0545250. We are greatly indebted to many colleagues who furnished MT and earthquake data from the three study areas. Stephen Bannister and Donna Eberhart-Phillips provided seismic data from New Zealand. For the Himalaya, Martyn Unsworth furnished MT data and Larry Brown, Gaspar Monsalve, Jim Ni, Vera Schulte-Pelkum, Peter Shearer, and Francis Wu are all responsible for the seismic data that we received. Previous MT results for the San Andreas fault were furnished by Martyn Unsworth and Paul Bedrosian. Michael Becken, Steve Park, and Oliver Ritter graciously shared their new, unpublished MT data for the Parkfield area. Newly located hypocenters for the 2004 M=6.0 Parkfield earthquake and its aftershocks were provided by Jeanne Hardebeck. Discussions with Yuri Fialko and John Vidale proved to be very valuable. Hugh Bibby, Steve Day, Yuri Fialko, Rob Mellors, Steve Park, and Peter Shearer read early versions of the manuscript and made many constructive suggestions for improvement. Bruce Hobbs shared his recent 2-D geodynamic numerical models and answered several key questions regarding the results. We are solely responsible for any misunderstandings. We could not have handled the large earthquake data sets without full support from the University of California-San Diego, Scripps Institution of Oceanography's Visualization Center; Graham Kent and Tom Im answered the call. We also thank Tony Carrasco who worked tirelessly and cheerfully to provide many of the graphics. We greatly appreciated the efforts by reviewers Martyn Unsworth, James Connolly, and Fred Davey whose comments and suggestions improved the paper significantly. Finally, we thank the organizers of the Workshop on Geotectonic Investigation of a Modern Continent-Continent Collisional Oregon:

Southern Alps, NZ held in Christchurch, New Zealand in June 2005 since this paper grew out of that workshop.

REFERENCES

- Ague, J. J. (2006), Fluids in the deep crust and in subduction zones: Frontiers for research, *EOS Trans. AGU*, 87(36), Jt. Assem. Suppl. Abstract U23A-06.
- Anderson, J. L., R. H. Osborne, and D. E. Palmer (1983), Cataclastic rocks of the San Gabriel fault—an expression of deformation at deeper crustal levels in the San Andreas fault zone, *Tectonophysics*, 98, 209–251.
- Argus, D., and R. Gordon (2001), Present day motion across the Coast Range and San Andreas fault system in central California, *Geol. Soc. of Am. Bull.*, 113, 1580–1592.
- Arora, B., M. Unsworth, and G. Rawat (2007), Deep resistivity structure of the northwest Indian Himalaya and its tectonic implications, *Geophys. Res. Lett.*, 34, doi:10.1029/2006GL029165.
- Atwater, T., and J. M. Stock (1998), Pacific-North American plate tectonics of Neogene southwestern United States: An update: *Int. Geol. Rev.*, 40(5), 375–402.
- Bailey, R. C. (1990), Trapping of aqueous fluids in the deep crust, *Geophys. Res. Lett.*, 17(8), 1129–1132.
- Bailey, R. C. (1994), Fluid trapping in midcrustal reservoirs by H₂O-CO₂ mixtures, *Nature*, 371(6494), 238–240.
- Bakum, W. H., and A. G. Lindh (1985), The Parkfield, California, earthquake prediction experiment, *Science*, 229, 619–624.
- Bannister, S., C. Thurber, and J. Louie (2006), Detailed fault structure highlighted by finely relocated aftershocks, Arthur's Pass, New Zealand, *Geophys. Res. Lett.*, 33, doi:10.1029/2006GL027462.
- Beaumont, C. R., A. Jamieson, M. H. Nguyen, and B. Lee (2001), Himalayan tectonics explained by extrusion of a low-viscosity crustal channel coupled to focused surface denudation, *Nature*, 414, 738–742.
- Beavan, J., M. Moore, C. Pearson, M. Henderson, B. Parsons, S. Bourne, P. England, D. Walcott, G. Blick, D. Darby, and K. Hodgkinson (1999), Crustal deformation during 1994–1998 due to oblique continental collision in the central Southern Alps, New Zealand and implications for seismic potential of the Alpine fault, *J. Geophys. Res.*, 104, 25,233–25,255.
- Beavan, J., S. Ellis, L. Wallace, and P. Denys (this volume), Kinematic constraints from GPS on oblique convergence of the Pacific and Australian plates, central South Island, New Zealand.
- Becken, M., O. Ritter, S. K. Park, P. A. Bedrosian, U. Weckmann, and M. Weber (2006), A deep crustal fluid channel into the San Andreas fault system imaged by magnetotellurics, *EOS Trans. AGU*, 87(52), Fall Meet. Suppl., Abstract T21C-0436.
- Becken, M., O. Ritter, S. K. Park, P. A. Bedrosian, U. Weckmann, and M. Weber (2007), A deep crustal fluid channel into the San Andreas fault system near Parkfield, California, *Geophys. J. Int.*, in press.
- Bedrosian, P. A., M. J. Unsworth, and G. Egbert (2002), Magnetotelluric imaging of the creeping segment of the San Andreas fault near Hollister, *Geophys. Res. Lett.*, 29, doi: 2910.1029/2001GL014119.

- Bedrosian, P. A., M. J. Unsworth, G. D. Egbert, and C. H. Thurber (2004), Geophysical images of the creeping segment of the San Andreas fault: implications for the role of crustal fluids in the earthquake process, *Tectonophysics*, 385, 137–158.
- Brace, W. F., and J. D. Byerlee (1970), California earthquakes: Why only shallow focus? *Science*, 168(3939), 1573–1575.
- Brenan, J. M. (1991), Development and maintenance of metamorphic permeability: implications for fluid transport, in *Contact Metamorphism, Rev. Mineral.*, vol. 26, edited by D.M. Kerrick, pp. 291–319, Mineral. Soc. of Am., Washington, D.C.
- Byerlee, J. (1978), Friction of rocks, *Pure Appl. Geophys.*, 116, 615–626.
- Byerlee, J. (1990), Friction, overpressure and fault normal compression, *Geophys. Res. Lett.*, 17, 2109–2112.
- Byerlee, J. (1993), Model for episodic flow of high-pressure water in fault zones before earthquakes, *Geology*, 21, 303–306.
- Chen, W.-P., and Z. Yang (2004), Earthquakes beneath the Himalayas and Tibet: Evidence for Strong lithospheric mantle, *Science*, 304, 1949–1952.
- Chery, J., M. D. Zoback and R. Hassani (2001), An integrated mechanical model of the San Andreas fault in central and northern California, *J. Geophys. Res.*, 106, 22,051–22,066.
- Connolly, J. A. D., and A. B. Thompson (1989), Fluid and enthalpy production during regional metamorphism, *Contrib. Mineral. Petrol.*, 102, 346–366.
- Connolly, J. A. D. (1997), Devolatilization-generated fluid pressure and deformation-propagated fluid flow during metamorphism, *J. Geophys. Res.*, 102, 18,149–18,173.
- Connolly, J. A. D., and Y. Y. Podladchikov (2004), Fluid flow in compressive tectonic settings: implications for midcrustal seismic reflectors and downward fluid migration, *J. Geophys. Res.*, 109, doi:10.1029/2003JB002822.
- Cox, S. C., and R. H. Findlay (1995), The main divide fault zone and its role in the development of the Southern Alps, New Zealand, *N. Z. J. Geol. Geophys.*, 38, 489–499.
- Cox, S. F. (2005), Coupling between deformation, fluid pressures, and fluid flow in ore-producing hydrothermal systems at depth in the crust, in *Economic Geology 100th Anniversary Volume*, edited by J. W. Hedenquist, J. F. H. Thompson, R. J. Goldfarb, and J. P. Richards, *Econ. Geol.*, 39–76.
- Davey, F. J., T. Henyey, W. S. Holbrook, D. Okaya, T. A. Stern, A. Melhuish, S. Henrys, H. Anderson, D. Eberhart-Phillips, T. McEvilly, R. Uhrhammer, F. Wu, G. R. Jiracek, P. E. Wannamaker, G. Caldwell, and N. Christenson (1998), Preliminary results from a geophysical study across a modern, continent-continent collisional plate boundary - the Southern Alps, New Zealand: *Tectonophysics*, 288, 221–235.
- DeCelles, P. G., D. M. Robinson, and G. Zandt (2002), Implications of shortening in the Himalayan fold-thrust belt for uplift of the Tibetan Plateau, *Tectonics*, 21, 1062, doi: 10.1029/2001TC001322.
- DeMets, C., G. Gordon, D. F. Argus, and S. Stein (1994), Effect of recent revisions of the geomagnetic time scale on estimates of current plate motions, *Geophys. Res. Lett.*, 21, 2191–2194.
- Eaton, G. P. (1980), Geophysical and geological characteristics of the crust of the Basin and Range province, in *Continental Tectonics*, chm. B. C. Burchfiel, J. E. Oliver, and L. T. Silver, pp. 96–110, Nat. Res. Council, Washington.
- Eberhart-Phillips, D. (1995), Examination of seismicity in the central Alpine fault region, South Island, New Zealand, *N. Z. J. Geol. Geophys.*, 38, 571–578.
- Eberhart-Phillips, D., W. D. Stanley, B. D. Rodriguez, and W. J. Lutter (1995), Surface seismic and electrical methods to detect related faulting, *J. Geophys. Res.*, 100, 12,919–12,936.
- Eberhart-Phillips, D., and S. Bannister (2002), Three-dimensional crustal structure in the Southern Alps region of New Zealand from inversion of local earthquake and active source data, *J. Geophys. Res.*, 107(B10), 2262, doi:10.1029/2001JB000567.
- Famin, V., and S. Nakashima (2004), Fluid migration in fault zones and the evolution of detachments: The example of Tinos Island (Greece), in *Physicochemistry of Water in Geological and Biological Systems*, edited by S. Nakashima, C. J. Spiers, L. Mercury, P. A. Fenter, and M. F. Hochella Jr., Univ. Acad. Press, Tokyo, 189–209.
- Ferry, J. M. (1994), A historical review of metamorphic fluid flow, *J. Geophys. Res.*, 99, 15,487–15,498.
- Fialko, Y. (2004), Evidence of fluid-filled upper crust from observations of postseismic deformation due to the 1992 M_w 7.3 Landers earthquake, *J. Geophys. Res.*, 109, B08401, doi:10.1029/2004JB002985.
- Fyfe, W. S., N. J. Price, and A. B. Thompson (1978), *Fluids in the Earth's crust*, 383 pp., Elsevier, Amsterdam.
- Godfrey, N. J., G. S. Fuis, V. Langenheim, D. A. Okaya, and T. M. Brocher (2002), Lower crustal deformation beneath the central Transverse Ranges, southern California, *J. Geophys. Res.*, 107(B7), doi:10.1029/2001JB000354.
- Gonzalez, M. (2002), Magnetotelluric evidence for mid-crustal fluids in an active transpressive continental orogen, South Island, New Zealand, M.S. thesis, 151 pp., San Diego State Univ., San Diego, USA.
- Gough, D. I. (1986), Seismic reflectors, conductivity, water, and stress in the continental crust, *Nature*, 323, 143–144.
- Grapes, R. H., and T. Watanabe (1994), Mineral composition variation in Alpine Schist, Southern Alps, New Zealand: Implications for recrystallization and exhumation, *The Island Arc*, 3, 163–181.
- Gratier, J. P., P. Favreau, and F. Renard (2003), Modeling fluid transfer along California faults when integrating pressure solution crack sealing and compaction processes, *J. Geophys. Res.*, 108(B2), doi: 10.1029/2001JB000380.
- Groom, R. W., and R. C. Bailey (1989), Decomposition of magnetotelluric impedance tensor in the presence of local three-dimensional galvanic distortion, *J. Geophys. Res.*, 94, 1913–1925.
- Hickman, S., R. Sibson, and R. Bruhn (1995), Introduction to special issue: mechanical involvement of fluids in faulting, *J. Geophys. Res.* 100, 12,831–12,840.
- Hobbs, B. E., H. Tanaka, and Y. Iio (2002), Acceleration of slip motions in deep extensions of seismogenic faults in and below the seismogenic zone, *Earth Planets Space*, 54, 1195–1205.
- Hobbs, B. E., A. Ord, K. Regenauer-Lieb, and B. Drummond (2004), Fluid reservoirs in the crust and mechanical coupling between the upper and lower crust, *Earth Planets Space*, 56, 1151–1161.

- Hole, J. A., T. Ryberg, G. S. Fuis, F. Bleibinhaus, and A. K. Sharma (2006), Structure of the San Andreas fault zone at SA-FOD from seismic refraction survey, *Geophys. Res. Lett.*, *33*, doi: 10.1029/2005GL025194.
- Holness, M. B. (1993), Temperature and pressure dependence of quartz-aqueous fluid dihedral angles: The control of adsorbed H₂O on permeability of quartzites, *Earth Planet. Sci. Lett.*, *117*, 363–377.
- Holness, M. B. (1995), The effect of feldspar on quartz-H₂O-CO₂ dihedral angles at 4 kbar, with consequences for the behavior of aqueous fluids in migmatites, *Contributions to Mineralogy and Petrology*, *118*, 356–364.
- Holness, M. B. (1996), Surface chemical controls on pore-fluid connectivity in texturally equilibrated materials, in *Fluid Flow and Transport in Rocks: Mechanisms and Effects*, edited by B. D. Jamtveit and B.W.D. Yardley, pp. 149–170, Chapman and Hall, New York.
- Holness, M. B. (1998), Contrasting rock permeability in the aureole of the Ballachulish igneous complex, Scottish Highlands: The influence of surface energy, *Contrib. Mineral. Petrol.*, *131*, 86–94.
- Holness, M. B., and S. T. C. Siklos (2000), The rates and extent of textural equilibrium in high-temperature fluid-bearing systems, *Chem. Geol.*, *162*, 137–153.
- Iio, Y., and Y. Kobayashi (2002), A physical understanding of large intraplate earthquakes, *Earth Planets Space*, *54*, 1001–1004.
- Jiracek, G. R., E. P. Gustafson, and P. S. Mitchell (1983), Magnetotelluric results opposing magma origin of crustal conductors in the Rio Grande rift, *Tectonophysics*, *94*, 299–326.
- Jiracek, G. R., V. Haak, and K. H. Olsen (1995), Practical magnetotellurics in a continental rift environment, in *Continental Rifts: Evolution, Structure and Tectonics*, edited by K. H. Olsen, Elsevier, New York, 103–129.
- Jove, C. F., and R. G. Coleman (1998), Extension and mantle upwelling within the San Andreas fault zone, San Francisco Bay area, California, *Tectonics*, *17*, 883–890.
- Kennedy, B. M., Y. K. Kharaka, W. C. Evans, A. Allwood, D. J. DePaolo, J. Thordsen, G. Ambats, and R. H. Mariner (1997), Mantle fluids in the San Andreas fault system, *Science*, 1278–1281.
- Klemperer, S. L. (2006), Crustal flow in Tibet: Geophysical evidence for the physical state of Tibetan lithosphere, and inferred patterns of active flow, in *Channel flow, ductile extrusion and exhumation in continental collision zones*, edited by R. D. Law, M. P. Searle and L. Godin, *Geol. Soc. London Spec. Pub.*, *268*, 39–70.
- Koons, P. O., D. Craw, S. C. Cox, P. Upton, A. S. Templeton, and C. P. Chamberlain (1998), Fluid flow during active oblique convergence: A Southern Alps model from mechanical and geochemical observations, *Geology*, *26*, 159–162.
- Langin, W. R., L. D. Brown, and E. A. Sandvol (2003), Seismicity of central Tibet from project INDEPTH III seismic recordings, *Bull. Seismol. Soc. Am.*, *93*(5), 2146–2159.
- Ledo, J. (2005), 2-D versus 3-D magnetotelluric data interpretation, *Surveys Geophys.*, *26*, 511–543.
- Leitner, B., D. Eberhart-Phillips, H. Andersen, and J. L. Nabelek (2001), A focused look at the Alpine fault, New Zealand: Seismicity, focal mechanisms, and stress observations, *J. Geophys. Res.*, *106* (B2), 2193–2220.
- Lemonnier, C., G. Marquis, F. Perrier, J.-P. Avouac, G. Chitrakar, B. Kafle, S. Sapkota, U. Gautam, D. Tiwari, and M. Bano (1999), Electrical structure of the Himalaya of central Nepal: High conductivity around the mid-crustal ramp along the MHT, *Geophys. Res. Lett.*, *26*, 3261–3264.
- Li, S., M. J. Unsworth, J. R. Booker, W. Wei, H. Tan, and A. G. Jones (2003), Partial melt or aqueous fluid in the mid-crust of southern Tibet? Constraints from INDEPTH magnetotelluric data, *Geophys. J. Int.*, *153*, 289–304.
- Liu, Z., and P. Bird (2006), Two-dimensional and three-dimensional finite element modeling of mantle processes beneath central South Island, New Zealand, *Geophys. J. Int.*, *165*, 1003–1028.
- Mackie, R. L., D. W. Livelybrooks, T. R. Madden, and J. C. Larsen (1997), A magnetotelluric investigation of the San Andreas fault at Carrizo Plain California, *Geophys. Res. Lett.*, *24*, 1847–1850.
- Makovsky, Y., and S. L. Klemperer (1999), Measuring the seismic properties Tibetan bright-spots: Free aqueous fluids in the Tibetan middle crust, *J. Geophys. Res.*, *104*, 10,795–10,825.
- Marquis, G., and R. D. Hyndman (1992), Geophysical support for aqueous fluids in the deep crust: Seismic and electrical relationships, *Geophys. J. Int.*, *110*, 91–105.
- Manning, C. E., and S. E. Ingebritsen (1999), Permeability of the continental crust: Implications of geothermal data and metamorphic systems, *Rev. Geophys.*, *37*, 127–150.
- Monsalve, G., G., A. Sheehan, V. Schulte-Pelkum, S. Rajaure, M.R. Pandey, and F. Wu (2006), Seismicity and one-dimensional velocity structure of the Himalayan collision zone: Earthquakes in the crust and upper mantle, *J. Geophys. Res.*, *111*, doi:10.1029/2005JB004062.
- Nadeau, R. M., and D. Dolenc (2005), Nonvolcanic tremors deep beneath the San Andreas fault, *Science*, *307*, 389.
- National Research Council (1996), *Rock fractures and fluid flow: Contemporary understanding and applications*, National Academies Press, Washington, D.C.
- National Research Council (2003), *Living on an active Earth: Perspectives on earthquake science*, National Academies Press, Washington, D.C.
- Nelson, K. D., W. Zhao, L. D. Brown, J. Kuo, J. Che, X. Liu, S. L. Klemperer, Y. Makovsky, R. Meissner, J. Mechie, R. Kind, F. Wenzel, J. Ni, J. Nabelek, C. Leshou, H. Tan, W. Wei, A. G. Jones, J. Booker, M. Unsworth, W. S. F. Kidd, M. Hauch, D. Alsdorf, A. Ross, M. Cogan, C. Wu., E. Sandvol, and M. Edwards (1996), Partially molten middle crust beneath southern Tibet: Synthesis of Project INDEPTH results, *Science*, *274* (5293), 1684–1688.
- Norris, R. J. (2004), Strain localization within ductile shear zones beneath active faults: Alpine fault contrasted with the adjacent Otago fault system, New Zealand, *Earth Planets Space*, *56*, 1095–1101.
- Nur, A. and J. R. Booker (1972), Aftershocks caused by pore fluid pressure? *Science*, *175*, 885–877.
- Owens, T. J., and G. Zandt (1997), Implications of crustal property variations for models of Tibetan plateau evolution, *Science*, *387*, 37–43.

- Park, S. K., and J. J. Roberts (2003), Conductivity structure of the San Andreas fault, Parkfield, revisited, *Geophys. Res. Lett.*, *30*, doi:10.1029/2003GL017689.
- Pili, E., B. M. Kennedy, M. S. Conrad, and J. P. Gratier (1998), Isotope constraints on the involvement of fluids in the San Andreas fault, *Eos Trans. AGU*, *79*(17), S229–S230, Spring Meet. Suppl.
- Rice, J. R. (1992), Fault stress states, pore pressure distributions, and the weakness of the San Andreas fault, in *Fault Mechanics and Transport Properties of Rocks*, edited by B. Evans and T. F. Wong, pp. 475–503, Academic press, San Diego, CA.
- Rice, J. R., and M. Cocco (2007), Seismic fault rheology and earthquake dynamics, in *Tectonic Faults*, edited by M. R. Handy, G. Hirth, and N. Hovius, The MIT press, Cambridge, MA, 99–138.
- Ritter, O., A. Hoffmann-Rothe, P. A. Bedrosian, U. Weckmann, and V. Haak (2005), Electrical conductivity images of active and fossil fault zones, in *High Strain Zones: Structure and Physical Properties*, edited by D. Bruhn and L. Burini, *Geol. Soc., London, Spec. Publs.*, *245*, 165–186.
- Rodi, W., and R. L. Mackie (2001), Nonlinear conjugate gradients algorithm for 2-D magnetotelluric inversion, *Geophysics*, *66*, 174–187.
- Rogers, G., and H. Dragert (2003), Episodic tremor and slip on the Cascadia subduction zone: The chatter of silent slip, *Science*, *300*, 1942–1943.
- Royden, L. H., B. C. Burchfiel, R. W. King, E. Wang, Z. Chen, F. Shen, and Y. Li (1997), *Science*, *276*, 788–790.
- Sass, J. H., C. F. Williams, A. H. Lachenbruch, S. P. Galanis Jr., and F. V. Grubb (1997), Thermal regime of the San Andreas fault near Parkfield, *J. Geophys. Res.*, *102*(B12), 27,575–27,585.
- Scherwath, M., T. Stern, F. J. Davey, D. Okaya, W. S. Holbrook, R. Davies, and S. Kleffmann (2003), Lithospheric structure across oblique continental collision in New Zealand from wide-angle P wave modeling, *J. Geophys. Res.*, *108*(B12), doi:10.1029/2002JB002286.
- Schulte–Pelkum, V., M. Gaspar, A. Sheehan, M. R. Pandey, S. Sapkota, R. Biham, and F. Wu (2005), Imaging the Indian subcontinent beneath the Himalaya, *Nature*, doi:10.1038/nature03678.
- Shelly, D. R., G. C. Beroza, I. Satoshi, and S. Nakamura (2006), Low-frequency earthquakes in Shikoku, Japan, and their relationship to episodic tremor and slip, *Nature*, *442*, 188–191, doi:10.1038/nature04931.
- Sibson, R. H. (1984), Roughness at the base of the seismogenic zone: Contributing factors, *J. Geophys. Res.*, *89*(B7), 5791–5799.
- Sibson, R. H. (1992), Implications of fault-valve behavior for rupture nucleation and recurrence, *Tectonophysics*, *211*, 283–293.
- Spear, F. S. (1993), Metamorphic phase equilibria and pressure-temperature-time paths, *Miner. Soc. Amer. Monograph*, *1*, Washington, D. C., 799 p.
- Spratt, J. E., A. G. Jones, K. D. Nelson, M. J. Unsworth, and INDEPTH MT Team (2005), Crustal structure of the India-Asia collision zone, southern Tibet, from INDEPTH MT investigations, *Phys. Earth Planet. Inter.*, *150*, 227–237.
- Thompson, A. B., and J. A. D. Connolly (1990), Metamorphic fluids and anomalous porosities in the lower crust, *Tectonophysics*, *182*, 47–55.
- Thordsen, J. J., W. C. Evans, Y. K. Kharaka, B. M. Kennedy, and M. van Soest (2005), Chemical and isotopic composition of water and gases from the SAFOD wells: Implications to the dynamics of the San Andreas fault near Parkfield, *Eos Trans. AGU*, *86*(52), Fall Meet. Suppl., Abstract T23E-08.
- Thurber, C., S. Roecker, W. Ellsworth, Y. Chen, W. Lutter, and R. Sessions (1997), Two-dimension image of the San Andreas fault in the Northern Gabilan Range, central California, *Geophys. Res. Lett.*, *24*, 1591–1594.
- Thurber, C., H. Zhang, F. Waldhauser, J. Hardebeck, A. Michael, and D. Eberhart-Phillips (2006), Three-dimensional compressional wavespeed model, earthquake relocations, and focal mechanisms for the Parkfield, California, region, *Bull. Seism. Soc. Am.*, *96*, S38–S49.
- Tullis, J., A. Yund, and J. Farver (1996), Deformation-enhanced fluid distribution in feldspar aggregates and implications for ductile shear zones, *Geology*, *24*, 63–66.
- Unsworth, M. J., P. E. Malin, G. D. Egbert, and J. R. Booker (1997), Internal structure of the San Andreas fault at Parkfield, California, *Geology*, *25*, 359–362.
- Unsworth, M., G. Egbert, and J. Booker (1999), High-resolution imaging of the San Andreas fault in central California, *J. Geophys. Res.*, *104*(B1), 1131–1150.
- Unsworth, M., and P. A. Bedrosian (2004a), Electrical resistivity structure at the SAFOD site from magnetotelluric exploration, *Geophys. Res. Lett.*, *31*, doi:10.1029/2003GL019405.
- Unsworth, M., and P. A. Bedrosian (2004b), On the geoelectric structure of major strike-slip faults and shear zones, *Earth Planets Space*, *56*, 1177–1184.
- Unsworth, M. J., A. G. Jones, W. Wei, G. Marquis, S. Gokarn, J. E. Spratt and the INDEPTH-MT team (2005), Crustal rheology of the Himalaya and southern Tibet inferred from magnetotelluric data, *Nature*, *438*, doi:10.1038/nature04154.
- Upton, P., and P. O. Koons (this volume), Three-dimensional geodynamic framework for the Central Southern Alps, New Zealand: Integrating geology, geophysics and mechanical observations.
- Upton, P., D. Craw, T. G. Caldwell, P. O. Koons, Z. James, P. E. Wannamaker, G. R. Jiracek, and C. P. Chamberlain (2003), Upper crustal fluid flow in the outboard region of the Southern Alps, New Zealand, *Geofluids*, *3*, 1–12.
- van Avendonk, H. J. A., W. S. Holbrook, D. Okaya, J. K. Austin, F. Davey, and T. Stern (2004), Continental crust under compression: A seismic refraction study of South Island Geophysical Transect I, South Island, New Zealand, *J. Geophys. Res.*, *109*(B6), B06302.
- Vry, J. K., R. Maas, T. A. Little, D. Phillips, R. Grapes, and M. Dixon (2004), Zoned (Cretaceous and Cenozoic) garnets and the timing of high-grade metamorphism, Southern Alps, New Zealand, *J. Metamorphic Geol.*, *22*, 137–157.
- Vry, J. K., A. C. Storkey, and C. Harris (2001), Role of fluids in metamorphism of the Alpine fault zone, New Zealand, *J. Metamorphic Geol.*, *19*, 21–31.
- Walcott, R. I. (1998), Modes of oblique compression: Late Cenozoic tectonics of the South Island of New Zealand, *Rev. Geophys.*, *36*, 1–26.

- Wannamaker, P. E. (2005), Anisotropy versus heterogeneity in continental solid earth electromagnetic studies: fundamental response characteristics and implications for physicochemical state, *Surveys in Geophys.*, *26*, 733–765.
- Wannamaker, P. E., G. W. Hohmann, and S. H. Ward (1984), Magnetotelluric responses of three-dimensional bodies in layered earths, *Geophysics*, *49*, 1517–1534.
- Wannamaker, P.E., G. R. Jiracek, J. A. Stodt, T. G. Caldwell, V. M. Gonzalez, J. D. McKnight, and A. D. Porter (2002), Fluid generation and pathways beneath an active compressional orogen, the New Zealand Southern Alps, inferred from magnetotelluric data, *J. Geophys. Res.*, *107*(B6), doi:10.1029/2001JB000186.
- Watson, E. B., and J. M. Brenan (1987), Fluids in the lithosphere, 1, Experimentally determined wetting characteristics of CO₂-H₂O fluids and their implications for fluid transport, host rock physical properties, and fluid inclusion formation, *Earth Planet. Sci. Lett.*, *85*, 497–515.
- Watson, E. B., J. M. Brenan, and D. R. Baker (1990), Distribution of fluids in the continental mantle, in *Continental Mantle*, edited by M. A. Menzies, pp. 111–125, Clarendon Press, Oxford.
- Wei, W., M. Unsworth, A. Jones, J. Booker, H. Tan, D. Nelson, L. Chen, S. Li, K. Solon, P. Bedrosian, S. Jin, M. Deng, J. Ledo, D. Kay, and B. Roberts (2001), Detection of widespread fluids in the Tibetan crust by magnetotelluric studies, *Science*, *292*, 716–718.
- Yoshino, T., K. Mibe, A. Yasuda, and T. Fujii (2002), Wetting properties of anorthite aggregates: implications for fluid connectivity in continental lower crust, *J. Geophys. Res.*, *107*(B1), doi: 10.1029/2001JB000440.
- Zandt, G., and C. R. Carigan (1993), Small-scale convectivity instability and upper mantle viscosity under California, *Science*, *261*, 460–463.
- Zhang, P.-Z., Z. Shen, M. Wang, W. Gan, R. Burgmann, P. Molnar, O. Wang, Z. Niu, J. Sun, J. Wu, S. Hanrong, and Y. Xinzhao (2004), Continuous deformation of the Tibetan Plateau from global position system data, *Geology*, *32*(9), doi:10.1130/G20554.1, 808–812.

V. M. Gonzalez and G. R. Jiracek, Department of Geological Sciences, San Diego State University, San Diego, CA, USA.

T. G. Caldwell, GNS Science, Lower Hutt, New Zealand.

P. E. Wannamaker, Energy & Geoscience Institute, University of Utah, Salt Lake City, UT, USA.

D. Kilb, Scripps Institution of Oceanography, University of California, San Diego, La Jolla, CA, USA.